Chemistry and Physics Faculty Articles   Department of Chemistry and Physics

11-1992

Renormalization-Group Study of the Standard Model and its Extensions: The Standard Model

H. Arason
University of Florida

Diego Castano
University of Florida, castanod@nova.edu

B. Kesthelyi
University of Florida

S. Mikaelian

E. J. Piard
University of Florida

See next page for additional authors

Follow this and additional works at: http://nsuworks.nova.edu/cnso_chemphys_facarticles

Part of the Physics Commons

Authors

H. Arason, Diego Castano, B. Kesthelyi, S. Mikaelian, E. J. Piard, P. Ramond, and B. D. Wright

Renormalization-group study of the standard model and its extensions: The standard model

H. Arason, D. J. Castaño, B. Kesthelyi, S. Mikaelian, E. J. Piard, P. Ramond,
and B. D. Wright

Institute for Fundamental Theory, Department of Physics, University of Florida, Gainesville, Florida 32611
(Received 12 December 1991)

In this paper we present a comprehensive analysis of the running of *all* the couplings of the standard model to two loops, including threshold effects. Our purpose is twofold—to determine what the running of these parameters may indicate for the physics of the standard model and to provide a template for the study of its extensions up to the Planck mass.

PACS number(s): 12.10.Dm, 12.15.Ff, 14.80.Dq, 14.80.Gt

I. INTRODUCTION

The standard model, by meeting all confrontations with experiments, stands as a remarkably simple parametrization of known physics down to a scale of tenths of millifermis. Yet, it has many unsatisfactory aspects such as a large number of parameters, a triplication of chiral families, and three distinct gauge structures. Consequently, it is almost a creed among right thinking theorists that there must exist a much simpler underlying structure of which the standard model is a chiral shard. Many think that such a structure will make its appearance at much smaller scales, somewhere in the unexplored region between millifermis and the Planck scale. Experimentalists can only proceed one or two orders of magnitude at a time in their exploration of those scales. Theorists, on the other hand, are only limited by their imagination. Their approach for divining this structure is twofold. In the first, the quantum numbers of the standard model are grouped into mathematically pleasing structures, resulting in an exercise in quantum number pattern recognition. This has led to the early grand unified theories (GUT's) [1]. The second approach [2] is to use the renormalization group to extrapolate the standard model parameters to the unexplored scales. The purpose is to find if those parameters satisfy interesting relations at shorter distances. When used in conjunction with the former approach, this can give powerful hints of the physics expected at shorter scales. Of course, it all depends on having accurate data to input as initial conditions on the renormalization-group equations, as well as a strong theoretical basis for the evolution equations themselves. The minimal SU(5) GUT is the prototype for such analyses [3]. There, properties of the model at energies of order 10^{15} GeV are translated with the aid of the renormalization group to a prediction for proton decay that is not consistent with experiment. Data on the coupling constants are now sufficiently precise to rule out most simple GUT's, including SU(5), because of the absence of unification of the running couplings (GUT triangle) [4]. The same analysis has recently improved the feasibility of the supersymmetric extensions of these GUT's.

More recently, constraints coming from Yukawa coupling unification in supersymmetric SU(5) and SO(10) models have led to bounds on the mass of the top quark [5, 6]. Renormalization-group methods are of enduring practical importance in the attempts of high-energy physicists to glean indications of more fundamental theories from radiative corrections. For this reason we seek to provide a general guide for the search for patterns in renormalization-group analyses so that these techniques will be accessible to a wider audience of physicists.

We therefore collect in a comprehensive manner and in one place the necessary tools for making renormalization-group analyses of the standard model and of its various extensions. Some facets of this study have been addressed in the literature, albeit not all in the same place. We view this *compendium* as a template for general applications of the running of parameters from 1 GeV to Planck mass M_{Pl} upon which standard model extensions may be added. With the ever increasing precision of experiment, we expect the inclusion of two-loop effects to be crucial. Therefore we work to two-loop order and, moreover, include the complete Yukawa sector contribution, as well as treat properly the effects of thresholds. These last two points, we believe, constitute an improvement over previous efforts. We use numerical methods to evolve the parameters to different scales using the β functions found in the literature [7] and plot the results for representative values of the Higgs boson and top-quark masses.

A review of initial data extraction from experiments is presented in Sec. II. Many excellent reviews may be found in the literature, e.g., Marciano's [8] or Peccei's [9]. For completeness the section begins with a basic introduction to renormalization and renormalization scheme dependence. We go on to identify the values of the various parameters at the different scales where they are most accurately known. The determination of the electroweak gauge couplings is discussed in Sec. II B. We cover some of the ambiguities and uncertainties associated with the extraction of the strong coupling constant in Sec. II C.

The running of the quark and lepton masses and of the Cabibbo-Kobayashi-Maskawa (CKM) angles is generally

given through the running of the Yukawa matrices (even to one loop). We run the quark masses and CKM angles by diagonalizing the Yukawa matrices at every step in the Runge-Kutta method used in solving the β functions. However, in the literature, some authors write down analytic expressions for the running of these masses and angles by making some approximations. Typically, it is assumed that the contribution of the Yukawa couplings matrix is given essentially by the top-quark Yukawa coupling since it is much larger than the others. Sometimes a better approximation is made by keeping only the diagonal entries. Our numerical technique represents a minor improvement over these methods. Initial data extraction of the Yukawa couplings and the CKM angles is discussed in Sec. II D.

The extraction of the quark masses from data is discussed in Sec. II E. This is a complex issue well known to be marred by the nonperturbative nature of QCD. Hence, in the low-energy regime, we consider it necessary to include the pure QCD three-loop contribution to our analysis of the running of the quark masses. Initial data for lepton masses follow in Sec. II F. In Sec. II G we consider the extraction of and constraints on the physical top-quark and Higgs-boson masses. We address the scale dependence of the renormalized scalar vacuum expectation value in Sec. II H. Finally, the method used to obtain the values of all running parameters at the same initial scale is described in Appendix C. Readers familiar with these matters may wish to skip the relevant sections.

In Sec. III, we discuss how threshold effects are incorporated into our analysis. It is well known that in the context of GUT's the effects of particle thresholds are of great importance in analyzing their low-energy predictions, [10–14] such as decreasing the naive estimate of the proton lifetime [10]. For completeness we present a detailed analysis of threshold effects in the standard model where these effects are numerically less important; the two-loop effects dominate the effects of the electroweak threshold. This work is of theoretical interest because the same methods are applicable to other models. Also we include threshold effects in the running fermion masses, an analysis absent from the present literature.

A quantitative analysis of our results makes up Sec. IV. We contrast the effects of using one-loop versus two-loop β functions and of including a proper versus a naive treatment of thresholds. We include plots of all the running parameters over the entire range of mass scales and also use these plots to display the effects discussed. Furthermore we present some tables with actual numerical differences associated with these effects.

II. INITIAL VALUE EXTRACTION FROM DATA

A. Renormalization scheme

Renormalization is a reparametrization of a theory which renders Green's functions and physical quantities finite order by order in perturbation theory. A specific choice of renormalized parameters defines a renormalization scheme. The physics is, of course, independent of

how the theory is renormalized. A common way of relating bare and renormalized parameters is

$$g_0 = g - \delta g , \qquad (2.1)$$

where g_0 is the bare parameter, g is the renormalized parameter, and δg is the counterterm. Fixing the counterterms by requiring them to consist only of the infinite terms needed to render the theory finite defines the minimal subtraction (MS) prescription [15]. A feature of the MS scheme is a mass scale μ which enters in the process of regularizing divergent integrals using dimensional regularization. Furthermore, the unit of mass μ is used to keep couplings dimensionless when continuing to d dimensions in the dimensional regularization procedure. For example, if Eq. (2.1) represents any of the three gauge couplings of the standard model, then μ is introduced as follows to keep them dimensionless:

$$g_0(\varrho\mu)^{-\epsilon} = g - \delta g , \qquad (2.2)$$

where ϱ is a constant parametrizing the arbitrariness in the finite parts of divergent integrals in dimensional regularization, and $\epsilon = (4 - d)/2$. Equation (2.2) defines a family of MS schemes. Choosing $\varrho = 1$ is the simplest MS scheme which was described above. Choosing $\varrho^2 = e^{\gamma_E}/4\pi$, where $\gamma_E = 0.5722\ldots$ is the Euler-Mascheroni constant, defines the so-called modified minimal subtraction ($\overline{\text{MS}}$) prescription [16]. This scheme is the most commonly employed in QCD calculations, and it is the one we adopt. The free parameters of the standard model in the $\overline{\text{MS}}$ schemes are μ dependent. Their μ evolution is governed by the β functions of the renormalization group. Moreover, these running parameters are not in general equal to their corresponding physical values (consequently, for the masses, we adopt a convention wherein upper case M's refer to physical values and lower case m's denote $\overline{\text{MS}}$ values). This is to be contrasted with the on-shell renormalization scheme in which, for example, the renormalized masses equal their physical values and the renormalized electromagnetic coupling equals the fine structure constant. However, the MS schemes have the attractive characteristic that the β functions are μ independent and therefore particularly simple to integrate. Physical quantities $P[\{g_i(\mu)\}, \mu]$ expressed in terms of μ and the running parameters of the theory, $\{g_i(\mu)\}$, must be μ independent

$$\mu\frac{d}{d\mu}P[\{g_i(\mu)\}, \mu] = \left(\mu\frac{\partial}{\partial\mu} + \beta_i\frac{\partial}{\partial g_i}\right)P = 0 , \quad (2.3)$$

where the β_i are the β functions. The two-loop β functions of the standard model have been collected in Appendix A.

As mentioned above physical quantities are renormalization scheme independent. However, this assumes that calculations can be done without approximation. In reality, calculations are only perturbative approximations and these do depend on the renormalization scheme. In QCD where the strong coupling α_s is large, there will be renormalization scheme dependence problems. In the electroweak model, as in QED where the couplings are

small, this is not so great a problem.

We now turn in the following subsections to the issue of extracting initial data for the standard model parameters.

B. $\alpha_1(M_Z)$ and $\alpha_2(M_Z)$

The determination of the $SU(2)_L \times U(1)_Y$ couplings proceeds from the standard model relations

$$\alpha_1(\mu) \equiv \frac{g_1^2(\mu)}{4\pi} = C^2 \frac{\alpha(\mu)}{\cos^2\theta_W(\mu)} ,$$

$$\alpha_2(\mu) \equiv \frac{g_2^2(\mu)}{4\pi} = \frac{\alpha(\mu)}{\sin^2\theta_W(\mu)} , \qquad (2.4)$$

where $\alpha(\mu) = e^2(\mu)/4\pi$ and C^2 is a normalization constant which equals 1 for the standard model and equals $\frac{5}{3}$ when the standard model is incorporated in grand unified theories of the $SU(N)$ and $SO(N)$ type [2]. What is required to specify these couplings are the values of $\alpha(\mu)$ and $\sin^2\theta_W(\mu)$ in the renormalization scheme we employ (i.e., $\overline{MS}$). The electromagnetic fine structure constant ($\alpha_{em}^{-1} \approx 137.036$) is extrapolated from zero momentum scale to a scale μ equal to M_Z in our case. In pure QED with one species of fermion with mass m, the $\overline{MS}$ renormalized vacuum polarization function is given by

$$\Pi(q^2) = \frac{\alpha(\mu)}{3\pi} \left[\ln \frac{\mu^2}{m^2} - 6 \int_0^1 dx\, x(1-x) \right.$$
$$\left. \times \ln\left(1 - x(1-x)\frac{q^2}{m^2}\right) \right] . \qquad (2.5)$$

The renormalized coupling $\alpha(\mu)$ is related to the fine structure constant α_{em} as follows:

$$\alpha_{em} = \frac{\alpha(\mu)}{1 + \Pi(0)} . \qquad (2.6)$$

In the standard model where there are many species of charged fermions and charged gauge bosons, Eq. (2.6) generalizes to [17]

$$\alpha^{-1}(\mu) = \alpha_{em}^{-1} - \frac{2}{3\pi} \sum_f Q_f^2 \ln \frac{\mu}{m_f} \theta(\mu - m_f) + \frac{1}{6\pi} . \qquad (2.7)$$

The effects of the strong interaction which enter as a hadronic contribution to the vacuum polarization function must be included also. The nonperturbative nature of the strong interaction at low momentum is handled by rewriting the hadronic contribution to the vacuum polarization at zero momentum as

$$\Pi^h(0) = [\Pi^h(0) - \Pi^h(q^2)] + \Pi^h(q^2) . \qquad (2.8)$$

If q^2 is chosen large enough, $\Pi^h(q^2)$ can be calculated perturbatively. The terms $[\Pi^h(0) - \Pi^h(q^2)]$ can then be related to the total cross section for $e^+e^- \to$ hadrons [17]. Using the optical theorem, we can write

$$\text{Im}\{\Pi^h(s)\} = \frac{s}{4\pi\alpha_{em}} \sigma(e^+e^- \to \text{hadrons}) , \qquad (2.9)$$

where s is the square of the center-of-mass energy. For the process $e^+e^- \to \mu^+\mu^-$, the cross section is calculated to be (taking $m_\mu = 0$)

$$\sigma(e^+e^- \to \mu^+\mu^-) = \frac{4\pi\alpha_{em}^2}{3s} . \qquad (2.10)$$

In terms of the ratio of these two cross sections,

$$R(s) = \frac{\sigma(e^+e^- \to \text{hadrons})}{\sigma(e^+e^- \to \mu^+\mu^-)} , \qquad (2.11)$$

we can write Eq. (2.9):

$$\text{Im}\{\Pi^h(s)\} = \frac{\alpha_{em}}{3} R(s) . \qquad (2.12)$$

Using an unsubtracted dispersion relation $\Pi^h(q^2)$, the combination $[\Pi^h(0) - \Pi^h(q^2)]$ can be expressed as

$$\Pi^h(0) - \Pi^h(q^2) = \frac{q^2\alpha_{em}}{3\pi} \int_{4m_\pi^2}^\infty ds\, \frac{R(s)}{s(q^2 - s)} . \qquad (2.13)$$

This can be evaluated using experimentally known data. This procedure yields a value

$$\alpha^{-1}(M_Z) = 127.9 \pm 0.3 . \qquad (2.14)$$

The process independent, renormalized weak mixing angle $\sin^2\theta_W$ of the on-shell scheme is defined to be

$$\sin^2\theta_W \equiv 1 - \frac{M_W^2}{M_Z^2} , \qquad (2.15)$$

where M_W and M_Z are the physical masses of the W and Z gauge bosons. Knowing the precise values of the W- and Z-boson masses and using the equation above provides one way of extracting the value of $\sin^2\theta_W$. Alternatively, the bare relation involving the low-energy Fermi constant measured in muon decay and the W-boson mass,

$$\frac{G_{\mu 0}}{\sqrt{2}} = \frac{e_0^2}{8\sin^2\theta_{W0} M_{W0}^2} , \qquad (2.16)$$

may be corrected to order α and rewritten [18, 19]

$$M_W = M_Z \cos\theta_W = \left(\frac{\pi\alpha_{em}}{\sqrt{2}G_\mu}\right)^{\frac{1}{2}} \frac{1}{\sin\theta_W (1 - \Delta r)^{\frac{1}{2}}} , \qquad (2.17)$$

with $(\pi\alpha_{em}/\sqrt{2}G_\mu)^{\frac{1}{2}} = 37.281$ GeV and Δr is a parameter containing order α radiative corrections and which depends on the mass of the top quark and Higgs boson. We can view the radiative corrections represented by Δr as accounting for the mismatch in the scales associated with the parameters of the relation. G_μ and α_{em} are low-energy parameters whereas M_W and $\sin^2\theta_W$ are associated with the electroweak scale. We can absorb the radiative effects using the renormalization group by replacing G_μ and α_{em} with corresponding running parameters at M_Z:

$$\frac{\pi\alpha(M_Z)}{\sqrt{2}G_\mu(M_Z)M_W^2\sin^2\theta_W} \approx 1 \ . \qquad (2.18)$$

Combining Eqs. (2.17) and (2.18) gives

$$\Delta r \approx 1 - \frac{\alpha_{\rm em}}{\alpha(M_Z)}\frac{G_\mu(M_Z)}{G_\mu} \ . \qquad (2.19)$$

Using Eq. (2.7) and the fact that $G_\mu(M_Z) \approx G_\mu$ (see Sec. II H) gives an estimate of the size of the radiative corrections

$$\Delta r \approx 0.07 \ . \qquad (2.20)$$

For large values of M_t and M_H $(M_t, M_H \gg M_Z)$ [18, 20],

$$\Delta r \approx 1 - \frac{\alpha_{\rm em}}{\alpha(M_Z)} - \frac{3\alpha_{\rm em}}{16\pi\sin^4\theta_W}\frac{M_t^2}{M_Z^2}$$
$$+ \frac{11\alpha_{\rm em}}{48\pi\sin^2\theta_W}\ln\frac{M_H^2}{M_Z^2} \ . \qquad (2.21)$$

A third way of extracting $\sin^2\theta_W$ is from neutral-current experiments, among which deep-inelastic neutrino scattering appears to provide the best determination. A running $\sin^2\theta_W(\mu)$ may be defined in $\overline{\rm MS}$ and differs from the above $\sin^2\theta_W$ by order α corrections. The $\overline{\rm MS}$ running W-boson mass $m_W(\mu)$ and the corresponding physical mass M_W, identified as the simple pole at $q^2 = M_W^2$ of the W propagator, are related as

$$M_W^2 = m_W^2(\mu) + A_{WW}^T(M_W^2, \mu) \ , \qquad (2.22)$$

where A_{WW}^T is the transverse part of the W self-energy. A similar relation holds for the Z boson. In $\overline{\rm MS}$ renormalization, the following relation defines the running $\sin^2\theta_W(\mu)$:

$$\sin^2\theta_W(\mu) = 1 - \frac{m_W^2(\mu)}{m_Z^2(\mu)} \ . \qquad (2.23)$$

Equation (2.22) and its Z analogue may be combined with Eq. (2.23) to give

$$\frac{\sin^2\theta_W(\mu)}{\sin^2\theta_W} = 1 - \frac{\cos^2\theta_W}{\sin^2\theta_W}\left(\frac{A_{ZZ}^T(M_Z^2, \mu)}{M_Z^2}\right.$$
$$\left. - \frac{A_{WW}^T(M_W^2, \mu)}{M_W^2}\right) \ . \qquad (2.24)$$

An explicit expression relating $\sin^2\theta_W$ and $\sin^2\theta_W(M_W)$ is given in Ref. [21].

Another relation for $\sin^2\theta_W(\mu)$ may be arrived at directly linking it to M_Z [22] or M_W [23]. In particular, if one chooses M_W as the input mass, then one introduces a radiative correction parameter $\Delta\hat{r}_W$ such that

$$\sin^2\theta_W(M_Z)(1 - \Delta\hat{r}_W) = \sin^2\theta_W(1 - \Delta r) \ , \qquad (2.25)$$

from which it follows that

$$\sin^2\theta_W(M_Z) = \frac{(37.271)^2}{M_W^2(1 - \Delta\hat{r}_W)} \ . \qquad (2.26)$$

Similarly one can introduce a radiative correction $\Delta\hat{r}_Z$ if one chooses M_Z as the input mass

$$\sin^2\theta_W(M_Z)\cos^2\theta_W(M_Z)(1 - \Delta\hat{r}_Z)$$
$$= \sin^2\theta_W\cos^2\theta_W(1 - \Delta r) \ . \qquad (2.27)$$

A fit to all neutral-current data gives

$$\sin^2\theta_W(M_Z) = 0.2324 \pm 0.0011 \ , \qquad (2.28)$$

for arbitrary M_t [24]. Using these values of $\alpha(M_Z)$ and $\sin^2\theta_W(M_Z)$ yields

$$\begin{aligned} \alpha_1(M_Z) &= 0.016\,98 \pm 0.000\,09 \ , \\ \alpha_2(M_Z) &= 0.033\,64 \pm 0.0002 \ . \end{aligned} \qquad (2.29)$$

C. $\alpha_s(M_Z)$

The value of the strong coupling is known with less precision than most of the parameters of the standard model. This is due to large theoretical uncertainties arising from the nonperturbative nature of low-energy QCD and the slow convergence of perturbation series in high-energy QCD. Moreover, this uncertainty is hard to quantify.

In the extraction of $\alpha_s = g_s^2/4\pi$ from a physical process many obstacles arise. Since the convergence of the QCD perturbation theory series is not very fast, one must check higher order effects. Even if one chooses processes which do not involve hadronization, a most delicate problem in the extraction of α_s comes from working to finite order in perturbation theory. Physical quantities should of course be renormalization scheme independent, but the necessity of approximation introduces dependence on the renormalization scheme. Typically, the same physical quantity calculated in two different schemes to the nth order of α_s will differ by terms of order α_s^{n+1}. As α_s is large, this difference may be large and thus may lead to renormalization scheme dependence problems. This problem manifests itself in the difficulty of choosing the renormalization scale μ to use for the particular experiment from which one is extracting the strong coupling. Ideally one would like to choose μ to minimize the unknown higher order terms, but that is of course not possible. Sometimes μ is approximated by the scale at which the highest order known term vanishes or by the scale at which that term gives a stationary prediction. However, the most frequent choice is $\mu = E$, where E is some characteristic energy scale of the experiment. This choice is plausible since it minimizes the typical terms that arise which involve $\ln(Q/\mu)$, with Q some momentum in the process, typically $\sim E$. All the processes from which the strong coupling is extracted suffer from this problem and thus each individual extraction of α_s has large uncertainties. To obtain the best estimate of the strong coupling we shall take together the results from different processes. These include e^+e^- scattering into hadrons, heavy quarkonium decay, scaling violations in deep inelastic lepton-hadron scattering, and jet production in e^+e^- scattering.

We first consider the extraction of α_s from e^+e^- scattering into hadrons. The cross section is, ignoring finite quark mass effects [25],

$$\sigma(e^+e^- \to \text{hadrons}) = \frac{4\pi\alpha_{\rm em}^2}{3s}3(1+z)\left(\sum_q e_q^2\right)\left[1+\frac{\alpha_s}{\pi}+A_2\left(\frac{\alpha_s}{\pi}\right)^2+A_3\left(\frac{\alpha_s}{\pi}\right)^3+O\left(\alpha_s^4\right)\right], \qquad (2.30)$$

where the effects from Z exchange have been put into the factor z. For $n_f = 5$ the numerical values of the coefficients are [26] $A_2 = 1.409$ and $A_3 = -12.805$. This determination of α_s has the advantage that it is inclusive, since there is no dependence on hadronization models. Its main drawback is that the effect is not very sensitive to α_s as the effect starts at zeroth order in α_s. The experimental error is relatively large and in fact dominates the theoretical error. The value of α_s has been extracted from the total cross section of e^+e^- into hadrons by Gorishny et al. [26] who find $\alpha_s(34 \text{ GeV}) \simeq 0.170\pm0.025$. As an estimate of the error coming from cutting off the perturbation series we use the size of the highest order correction and estimate the relative cutoff error to be $\simeq 13(\alpha_s/\pi)^2$. Thus we find $\alpha_s(34 \text{ GeV}) \simeq 0.170 \pm 0.025 \pm 0.006(\text{cutoff}) \simeq 0.170 \pm 0.026$, which using three-loop α_s and two-loop α running is equivalent to $\alpha_s(M_Z) \simeq 0.140 \pm 0.018$ (recent data from the CERN e^+e^- collider LEP [27] give essentially the same result).

The decay of heavy quarkonium is another process from which α_s can be extracted. The decay rates are sensitive to the strong coupling, the dominant modes going as α_s^2 or α_s^3, depending on the state of the $q\bar{q}$ system. The decay rates can be calculated in the nonrelativistic approximation. The rates themselves depend on the wave function amplitude at the origin, which is unknown but cancels out of branching ratios. The most useful of these branching ratios is [28]

$$\frac{\Gamma(\Upsilon\to\gamma GG)}{\Gamma(\Upsilon\to GGG)}=\frac{4}{5}\frac{\alpha_{\rm em}}{\alpha_s(M_b)}\left[1-2.6\frac{\alpha_s(M_b)}{\pi}\right], \qquad (2.31a)$$

$$\frac{\Gamma(\Upsilon\to GGG)}{\Gamma(\Upsilon\to\mu^+\mu^-)}=\frac{10}{9}\left(\frac{M_\Upsilon}{2M_b}\right)^2\frac{(\pi^2-9)\alpha_s^3(M_b)}{\pi\alpha_{\rm em}^2}$$
$$\times\left[1+0.43\frac{\alpha_s(M_b)}{\pi}\right], \qquad (2.31b)$$

and

$$\frac{\Gamma(J/\psi\to GGG)}{\Gamma(J/\psi\to\mu^+\mu^-)}=\frac{5}{8}\left(\frac{M_{J/\psi}}{2M_c}\right)^2\frac{(\pi^2-9)\alpha_s^3(M_c)}{\pi\alpha_{\rm em}^2}$$
$$\times\left[1+1.6\frac{\alpha_s(M_c)}{\pi}\right]. \qquad (2.31c)$$

The main uncertainty of this extraction of α_s is theoretical. The known higher order corrections are large so one expects the unknown corrections also to be large. In addition there are relativistic errors. Kwong et al. [28] have made a detailed analysis of α_s extraction from quarkonium decays. They find $\alpha_s(M_b) = 0.179 \pm 0.009$ from $\Gamma(\Upsilon\to\gamma GG)/\Gamma(\Upsilon\to GGG)$. They have also estimated the relativistic corrections and find $\alpha_s(M_b) = 0.189 \pm 0.008$ and $\alpha_s(M_c) = 0.29 \pm 0.02$ by looking at $\Gamma(\Upsilon\to GGG)/\Gamma(\Upsilon\to\mu^+\mu^-)$ and

$\Gamma(J/\psi\to GGG)/\Gamma(J/\psi\to\mu^+\mu^-)$. The errors given do not include the cutoff and relativistic errors. In their analysis Kwong et al. parametrized the relativistic corrections by a factor $(1+Cv^2/c^2)$ in the branching ratios. They found $C_1 \lesssim C \lesssim C_2$, with $C_1 \simeq -3.5$ and $C_2 \simeq -2.9$. Here $(v^2/c^2)_{J/\psi} = 0.24$ and $(v^2/c^2)_\Upsilon = 0.073$. We estimate the relativistic error to be $\simeq \alpha_s(M_b)(v^2/c^2)_\Upsilon(C_2-C_1)$. Similarly, we estimate the cutoff error by the highest order corrections in Eqs. (2.31a), (2.31b), and (2.31c). Using those estimates we find that α_s is most accurately determined from $\Gamma(\Upsilon\to GGG)/\Gamma(\Upsilon\to\mu^+\mu^-)$. We estimate the cutoff error to be $\approx \alpha_s(M_b)[0.43\,\alpha_s(M_b)/\pi] \simeq 0.005$ and the relativistic error to be $\alpha_s(M_b)(v^2/c^2)_\Upsilon(C_2-C_1) \simeq 0.008$ and conclude that $\alpha_s(M_b) = 0.189 \pm 0.008 \pm 0.005(\text{cutoff}) \pm 0.008(\text{relativistic}) = 0.189 \pm 0.012$. This value is equivalent to $\alpha_s(M_Z) = 0.111 \pm 0.005$.

Analysis of the structure functions in deep inelastic scattering gives a similar value for α_s. The strong coupling affects the way the structure functions vary with energy. These effects show up as logarithmic corrections to the exact Bjorken scaling predicted by the simple parton model. Like the other methods mentioned so far, the measurements of the structure functions do not depend on fragmentation and hadronization. The scaling violations in the structure functions have been measured with beams of electrons, muons, neutrinos, and antineutrinos on targets of hydrogen, deuterium, carbon, and iron among others. Martin et al. [29] have analyzed the most recent data and found $\alpha_s(M_Z) = 0.109 \pm 0.008$, including estimates of the truncation error.

Finally, we consider the extraction of α_s from e^+e^- scattering into jets. The production of multijets in e^+e^- scattering depends strongly on α_s. There, comparison of the QCD prediction and data introduces hadronization model dependence into the extraction of α_s. The evaluation of α_s is further complicated by dependence on cutoffs between different jets and the usual problems of the unknown higher order terms. To reduce the jet resolution problem, event shape variables, such as energy-energy correlations, the asymmetry of the energy-energy correlations, the oblateness, the thrust, etc., are used to extract α_s. As an example of an event shape variable we look at the energy-energy correlation (EEC) defined by [30]

$$\frac{1}{\sigma}\frac{d\Sigma^{\rm EEC}}{d\cos\chi}(\chi)=\frac{1}{\sigma}\sum_{i,j}\int\frac{d\sigma}{dy_idy_jd\cos\chi}y_iy_jdy_idy_j. \qquad (2.32)$$

The EEC can be experimentally constructed as

$$\frac{1}{N_{\rm events}}\sum_{\rm events}\sum_{i,j}y_iy_j\delta(\cos\theta_{ij}-\cos\chi), \qquad (2.33)$$

TABLE I. Values of α_s at M_Z and its error.

Process	α_s	$\Delta\alpha_s$
$e^+e^- \to$ hadrons	0.140	0.018
Υ decay	0.111	0.005
Deep-inelastic scattering	0.109	0.008
Jet distribution in e^+e^- scattering	0.115	0.008

where χ is the angle between calorimeter cells and $y_i = 2E_i/\sqrt{s}$ are the center-of-mass energy fractions of the detected particles. The asymmetry of the energy-energy correlation (AEEC) is defined as

$$\frac{1}{\sigma}\frac{d\Sigma^{\rm AEEC}}{d\cos\chi}(\chi) = \frac{1}{\sigma}\frac{d\Sigma^{\rm EEC}}{d\cos\chi}(\pi - \chi) - \frac{1}{\sigma}\frac{d\Sigma^{\rm EEC}}{d\cos\chi}(\chi) .$$

(2.34)

A perturbative calculation of the asymmetry gives [30]

$$\frac{1}{\sigma}\frac{d\Sigma^{\rm AEEC}}{d\cos\chi}(\chi) = \frac{\alpha_s}{\pi}A(\cos\chi)\left[1 + \frac{\alpha_s}{\pi}R(\cos\chi) + O(\alpha_s^2)\right] ,$$

(2.35)

with functions A and R calculated in perturbative QCD. The best data on the jet rates come from LEP. Recently those results have been extensively discussed in the literature [27, 31, 32]. Combining all the LEP data on jet distributions, including the full theoretical error, gives [27] $\alpha_s(M_Z) = 0.115 \pm 0.008$.

To summarize, the values of α_s and its error are given in Table I. To pick the value of $\alpha_s(M_Z)$ for our numerical studies we take the Gaussian weighted average of these values $([\sum(\alpha_s/\Delta\alpha_s^2)/\sum(1/\Delta\alpha_s^2)] \pm [\sum(1/\Delta\alpha_s^2)]^{-\frac{1}{2}})$, and we find [33] $\alpha_s(M_Z) = 0.113 \pm 0.004$.

D. Yukawa couplings

To take full account of the Yukawa sector in running all the couplings, initial values for the Yukawa couplings are necessary. They must be extracted from physical data such as quark masses and CKM mixing angles. Furthermore, the interesting parameters to be plotted must be determined step by step in the process of running to Planck mass. These two procedures are not unrelated and require the diagonalization of the up-type, down-type, and leptonic Yukawa matrices.

We use the convention of Machacek and Vaughn [7] where the interaction Lagrangian for the Yukawa sector is

$$\mathcal{L} = \overline{Q}_L\tilde{\Phi}\mathbf{Y}_u^\dagger u_R + \overline{Q}_L\Phi\mathbf{Y}_d^\dagger d_R + \overline{\ell}_L\Phi\mathbf{Y}_e^\dagger e_R + {\rm H.c.}$$

(2.36)

The Yukawa couplings are given in terms of 3×3 complex matrices. After electroweak symmetry breaking, these translate into the quark and lepton masses

$$\mathbf{Y}_e = \frac{\sqrt{2}}{v}\begin{pmatrix} m_e & 0 & 0 \\ 0 & m_\mu & 0 \\ 0 & 0 & m_\tau \end{pmatrix} ,$$

$$\mathbf{Y}_d = \frac{\sqrt{2}}{v}\begin{pmatrix} m_d & 0 & 0 \\ 0 & m_s & 0 \\ 0 & 0 & m_b \end{pmatrix} ,$$

(2.37)

$$\mathbf{Y}_u = \frac{\sqrt{2}}{v}\begin{pmatrix} m_u & 0 & 0 \\ 0 & m_c & 0 \\ 0 & 0 & m_t \end{pmatrix} V ,$$

where V is the CKM matrix which appears in the charged current

$$j_\mu^+ \sim \overline{u}_L\gamma_\mu V d_L.$$

(2.38)

It is a unitary 3×3 matrix often parametrized as

$$V = \begin{pmatrix} c_1 & s_1c_3 & s_1s_3 \\ -s_1c_2 & c_1c_2c_3 - s_2s_3e^{i\delta} & c_1c_2s_3 + s_2c_3e^{i\delta} \\ -s_1s_2 & c_1s_2c_3 + c_2s_3e^{i\delta} & c_1s_2s_3 - c_2c_3e^{i\delta} \end{pmatrix} ,$$

(2.39)

where $s_i = \sin\theta_i$ and $c_i = \cos\theta_i$, $i = 1, 2, 3$.

The entries of the parametrized CKM matrix can be related simply to the experimentally known CKM entries. The Particle Data Group [24] gives the following ranges of values (assuming unitarity) for the magnitudes of the elements of the CKM matrix:

$$|V| = \begin{pmatrix} 0.9747-0.9759 & 0.218-0.224 & 0.001-0.007 \\ 0.218-0.224 & 0.9734-0.9752 & 0.030-0.058 \\ 0.003-0.019 & 0.029-0.058 & 0.9983-0.9996 \end{pmatrix} .$$

(2.40)

These ranges of values can be converted to bounds for s_i, $i = 1, 2, 3$, and $\sin\delta$. We arrive at these bounds by finding values for the four angles such that the entries of the CKM matrix obtained from these satisfies the conditions imposed by Eq. (2.40). We find

$$0.2188 \le \sin\theta_1 \le 0.2235,$$
$$0.0216 \le \sin\theta_2 \le 0.0543,$$
$$0.0045 \le \sin\theta_3 \le 0.0290.$$

(2.41)

However the accuracy with which $|V|$ is known does not constrain $\sin\delta$. A set of angles $\{\theta_1, \theta_2, \theta_3, \delta\}$ was chosen that falls within the ranges quoted above. The initial data needed to run the Yukawa elements are extracted from the CKM matrix and the quark masses. A problem arises though for the mixing angles, which was solved for the quark masses (see Sec. II E), in that it is not clear at what scale the chosen initial values for these angles should be considered known. However, we have observed that for the whole range of initial values the running of the mixing angles is quite flat, with a perceptible increase in θ_2 between M_W and the Planck scale for higher top masses. This is in accordance with the angles being related to ratios of quark masses, and therefore, the exact knowledge of that scale (or lack thereof) is not as critical as might be feared *a priori*.

E. Known quark masses

As QCD is assumed to imply quark confinement, extraction of quark masses from experiment follows the same circuitous route as other QCD quantities such as α_s. In the past decade a variety of techniques has been developed and utilized to extract quark masses from the observed particle spectrum. Below, we shall briefly recount some such techniques. Furthermore, we shall present some values for the heavy quark masses based on the application of our numerical technique to three loops.

The light quark masses are the ones least accurately known. They are determined by a combination of chiral perturbation techniques and QCD spectral sum rules (QSSR's). In the former case the light quark masses are directly expressible in terms of the parameters of the explicit SU(2) and SU(3) chiral-symmetry breakings. One then considers an expansion of the form [34]

$$M_{\text{baryon}} = a + b\, m_{\text{light}} + \cdots \tag{2.42}$$

for the mass of a baryon from the $\frac{1}{2}^{+}$ octet and one of the form

$$M_{\text{meson}}^2 = B m_{\text{light}} + \cdots \tag{2.43}$$

for a typical member of the pseudoscalar octet. A parameter measuring the strength of the breaking of the more exact SU(2) chiral symmetry in comparison with the SU(3) one is the ratio

$$R = \frac{m_s - m'}{m_d - m_u} , \tag{2.44}$$

where

$$m' \equiv \frac{1}{2}(m_u + m_d) . \tag{2.45}$$

To lowest order in isospin splittings, this translates in the meson sector into

$$R = \frac{M_K^2 - M_\pi^2}{M_{K^0}^2 - M_{K^+}^2} , \tag{2.46}$$

and in the baryon sector into three different determinations of R:

$$R = \frac{\frac{1}{2}(M_\Xi - M_N) - \frac{3}{4}(M_\Sigma - M_\Lambda)}{M_n - M_p} ,$$
$$R = \frac{\frac{1}{2}(M_\Xi - M_N) + \frac{3}{4}(M_\Sigma - M_\Lambda)}{M_{\Xi^-} - M_{\Xi^0}} , \tag{2.47}$$
$$R = \frac{M_\Xi - M_N}{M_{\Sigma^-} - M_{\Sigma^+}} .$$

To make R compatible with all the above mass splittings one has to consider higher order corrections in Eqs. (2.42) and (2.43). Here infrared divergences emerge as one is expanding about a ground state containing Nambu-Goldstone bosons. Once such singularities are removed within the context of an effective chiral Lagrangian, one finds the optimum value of R:

$$R = 43.5 \pm 2.2 . \tag{2.48}$$

Together with the ratio [35]

$$\frac{m_s}{m'} = 25.7 \pm 2.6 , \tag{2.49}$$

also determined by applying Eq. (2.43) to the physical masses of π, η, and K, they imply the following renormalization-group-invariant mass ratio:

$$\frac{m_d - m_u}{2m'} = 0.28 \pm 0.03 . \tag{2.50}$$

QCD spectral sum rules are obtained in an attempt to relate the observed low-energy spectrum to the parameters describing the high-energy domain where perturbation theory becomes applicable to the quark-gluon picture [36, 40–42]. One starts by considering the two-point correlation functions for the vector $V_{ij}^\mu = \overline{\psi}_j \gamma^\mu \psi_i$ and axial vector $A_{ij}^\mu = \overline{\psi}_j \gamma^\mu \gamma_5 \psi_i$ quark currents

$$i \int d^4x\, e^{iq \cdot x} <0|T[V_{ij}^\mu(x)V_{ij}^{\nu\dagger}(0)]|0>$$

$$\equiv (q^\mu q^\nu - g^{\mu\nu}q^2)\Pi_{ij,V}^{(1)}(q^2) + q^\mu q^\nu \Pi_{ij,V}^{(0)}(q^2) , \tag{2.51}$$

$$i \int d^4x\, e^{iq \cdot x} <0|T[A_{ij}^\mu(x)A_{ij}^{\nu\dagger}(0)]|0>$$

$$\equiv (q^\mu q^\nu - g^{\mu\nu}q^2)\Pi_{ij,A}^{(1)}(q^2) + q^\mu q^\nu \Pi_{ij,A}^{(0)}(q^2) , \tag{2.52a}$$

where $i, j = u, d, s$ are the quark flavors. The current divergences satisfy

$$\partial_\mu V_{ij}^\mu(x) = i(m_i - m_j) :\overline{\psi}_i(x)\psi_j(x): ,$$
$$\partial_\mu A_{ij}^\mu(x) = i(m_i + m_j) :\overline{\psi}_i(x)\gamma_5\psi_j(x): . \tag{2.52}$$

The spectral functions $\text{Im}\{\Pi(q^2)\}$ obey certain sum rules based on how their analyticity properties are formulated. Among the QSSR's in vogue are the usual dispersion relations based on a Hilbert transform:

$$\Pi(q^2) = \frac{1}{\pi}\int_0^\infty dt \frac{\text{Im}\{\Pi(t)\}}{t + q^2} . \tag{2.53}$$

The Laplace transform sum rule is obtained by applying the inverse Laplace operator $\hat{L}$ to the last expression:

$$\hat{L}\Pi = \frac{\tau}{\pi}\int_0^\infty dt\, e^{-t\tau}\text{Im}\{\Pi(t)\} , \tag{2.54}$$

for τ a constant. The long-known finite energy sum rule (FESR) is obtained by applying the Cauchy theorem to $\Pi(z)$:

$$\frac{1}{\pi}\int_0^{q^2} dt\, t^n \text{Im}\{\Pi_{\text{theor}}(t)\} \simeq \frac{1}{\pi}\int_0^{q^2} dt\, t^n \text{Im}\{\Pi_{\text{expt}}(t)\} , \tag{2.55}$$

where n is any integer, and the moment sum rules are obtained by taking the nth derivative of Eq. (2.53):

$$\mathcal{M}^{(n)} \equiv \frac{(-1)^n}{n!}\frac{d^n}{(dq^2)^n}\Pi(q^2)$$

$$= \frac{1}{\pi}\int_0^\infty \frac{dt}{(t + q^2)^{n+1}}\text{Im}\{\Pi(t)\} . \tag{2.56}$$

The left-hand sides of Eqs. (2.53) through (2.56) follow from the high-energy calculations to which various perturbative and nonperturbative corrections have been found, while the right-hand sides represent the low-energy aspect, such as the hadronic vacuum polarization measured in $e^+e^- \rightarrow$ hadrons. Applied to the light quarks these sum rules imply [35]

$$\hat{m}_u + \hat{m}_d = 24.0 \pm 2.5 \text{ MeV} . \tag{2.57}$$

Together with Eq. (2.50) they reduce to

$$\hat{m}_u = 8.7 \pm 0.8 \text{ MeV} ,$$
$$\hat{m}_d = 15.4 \pm 0.8 \text{ MeV} . \tag{2.58}$$

The parameter $\hat{m}$ is a renormalization-group invariant which to three loops is related to the $\overline{\text{MS}}$ running mass parameter $m(\mu)$ via [38]

$$m(\mu) = \hat{m} \left(-\beta_1 \frac{\alpha_s}{\pi}(\mu) \right)^{-\gamma_1/\beta_1} \left\{ 1 + \frac{\beta_2}{\beta_1} \left(\frac{\gamma_1}{\beta_1} - \frac{\gamma_2}{\beta_2} \right) \frac{\alpha_s}{\pi}(\mu) + \frac{1}{2} \left[\frac{\beta_2^2}{\beta_1^2} \left(\frac{\gamma_1}{\beta_1} - \frac{\gamma_2}{\beta_2} \right)^2 - \frac{\beta_2^2}{\beta_1^2} \left(\frac{\gamma_1}{\beta_1} - \frac{\gamma_2}{\beta_2} \right) \right. \right.$$
$$\left. \left. + \frac{\beta_3}{\beta_1} \left(\frac{\gamma_1}{\beta_1} - \frac{\gamma_3}{\beta_3} \right) \right] \left(\frac{\alpha_s}{\pi}(\mu) \right)^2 \right\} , \tag{2.59}$$

where β_i and γ_i are the coefficients of the β functions for α_s and m given in Appendix A. From Eqs. (2.59) (to two loops) and (2.58) one may infer the values [35]

$$m_u(1 \text{ GeV}) = 5.2 \pm 0.5 \text{ MeV} ,$$
$$m_d(1 \text{ GeV}) = 9.2 \pm 0.5 \text{ MeV} . \tag{2.60}$$

In applying expression (2.58) it should be kept in mind that the continuity of $m(\mu)$ across a quark mass threshold requires $\hat{m}$ to depend on the effective number of flavors at the relevant scale, analogously to the QCD scale Λ. The strange quark mass is determined, averaging the value derived from Eqs. (2.57) and (2.49) with those obtained using Eq. (2.58) and the various QSSR values for $\hat{m}_u + \hat{m}_s$, to be [43]

$$\hat{m}_s = 266 \pm 29 \text{ MeV} , \tag{2.61}$$

corresponding to the running value

$$m_s(1 \text{ GeV}) = 194 \pm 4 \text{ MeV} . \tag{2.62}$$

For the heavier quarks, charm and bottom, one can make a more precise prediction. Here the nonrelativistic bound state approximation may be applied. The physical mass $M(q^2 = M^2)$ appearing in the Balmer series may be identified with the gauge and renormalization scheme invariant pole of the quark propagator:

$$S(q) = z(q)[\gamma \cdot q - M(q^2)]^{-1} . \tag{2.63}$$

Corresponding to the above pole mass is its Euclidean version $\overline{m}(-q^2)$, which, although renormalization-group invariant is not gauge invariant, and, therefore, not physical. The Euclidean mass parameter is the one often employed in the J/ψ and Υ sum rules, as it minimizes the radiative corrections in such sum rules. In the Landau gauge the two are related to two loops according to [36]

$$\overline{m}(M^2) = M(M^2) \left[1 - \frac{\alpha_s(M)}{\pi} \ln 4 \right] . \tag{2.64}$$

Once the pole mass is determined from the Euclidean one, the running mass at the pole mass is obtained to three loops via

$$m(q^2 = M^2) = \frac{M(q^2 = M^2)}{1 + \frac{4}{3} \frac{\alpha_s(M)}{\pi} + K \left(\frac{\alpha_s(M)}{\pi} \right)^2} , \tag{2.65}$$

where $K = 13.3$ for the charm and $K = 12.4$ for the bottom quarks [39].

From the J/ψ and Υ sum rules the following values have been extracted [35]:

$$\overline{m}_c(-q^2 = M_c^2) = 1.26 \pm 0.02 \text{ GeV} ,$$
$$\overline{m}_b(-q^2 = M_b^2) = 4.23 \pm 0.05 \text{ GeV} . \tag{2.66}$$

To obtain an accurate value for the corresponding pole masses, we applied the solution routine of Appendix C to Eq. (2.64), with the above values inserted and the three-loop β function for α_s given in Appendix A, to self-consistently obtain the pole masses

$$M_c(q^2 = M_c^2) = 1.46 \pm 0.05 \text{ GeV} ,$$
$$M_b(q^2 = M_b^2) = 4.58 \pm 0.10 \text{ GeV} . \tag{2.67}$$

Recently [37], new values for the charm and bottom pole masses have been extracted from CUSB and CLEO II by analysis of the heavy-light, B and B^*, D and D^* meson masses, and the semileptonic B and D decays with the results

$$M_c(q^2 = M_c^2) = 1.60 \pm 0.05 \text{ GeV} ,$$
$$M_b(q^2 = M_b^2) = 4.95 \pm 0.05 \text{ GeV} . \tag{2.68}$$

A weighted average of the values in Eqs. (2.67) and (2.68) yields

$$M_c(q^2 = M_c^2) = 1.53 \pm 0.04 \text{ GeV} ,$$
$$M_b(q^2 = M_b^2) = 4.89 \pm 0.04 \text{ GeV} . \tag{2.69}$$

The running masses at the corresponding pole masses then follow from Eq. (2.65):

$$m_c(M_c) = 1.22 \pm 0.06 \text{ GeV} ,$$
$$m_b(M_b) = 4.32 \pm 0.06 \text{ GeV} . \tag{2.70}$$

With these taken as initial data along with the value of the strong coupling at M_Z quoted in Sec. II C , we run (to three loops) the masses and α_s to obtain the following

values at the conventionally preferred scale of 1 GeV:

$$m_c(1 \text{ GeV}) = 1.41 \pm 0.06 \text{ GeV} ,$$

$$m_b(1 \text{ GeV}) = 6.33 \pm 0.06 \text{ GeV} . \qquad (2.71)$$

Our numerical approach does not make any more approximations than the ones assumed in the β functions and the mass equations used, apart from the approximation inherent in the numerical method itself, and, we therefore believe, is more in line with our program than using the "perturbatively integrated" form of the β functions. Thus we shall adopt the above values. It should be stressed that at the low scales under consideration the three-loop α_s corrections we have included in our mass and strong coupling β functions are often comparable to the two-loop ones and hence affect the accuracy of our final values noticeably. Nevertheless, it should be noted that the above expressions relating the various mass parameters are not fully loop consistent since to our knowledge Eq. (2.64) has only been computed to two loops.

In conclusion, it should be pointed out that although we opted for the QSSR extraction of masses, there are rival models, such as the nonperturbative potential models, which predict appreciably higher values of the heavy quark masses than the ones quoted here. These models, however, are not as fundamental as the approach considered here, and their connection to field theory is rather problematic.

F. Lepton masses

The physical (pole) masses of the leptons are very well known [24]:

$$M_e = 0.510\,999\,06 \pm 0.000\,000\,15 \text{ MeV} ,$$
$$M_\mu = 105.658\,387 \pm 0.000\,034 \text{ MeV} , \qquad (2.72)$$
$$M_\tau = 1.7841^{+0.0027}_{-0.0036} \text{ GeV} .$$

We use these values to determine initial data for the running masses. Some authors neglect QED corrections and use the physical values for the running values at $\sim M_Z$, which introduces only a small error. By calculating the one-loop self-energy corrections, one arrives at a QED relation between the running $\overline{\text{MS}}$ masses and the corresponding physical masses:

$$m_l(\mu) = M_l \left[1 - \frac{\alpha(\mu)}{\pi} \left(1 + \tfrac{3}{4} \ln \frac{\mu^2}{m_l^2} \right) \right] . \qquad (2.73)$$

Choosing $\mu = 1$ GeV as in the quark mass case and using Eqs. (2.73) and (2.7) yields the running lepton masses (taking $m_l = M_l$ in the log term above is an appropriate approximation to order α)

$$m_e(1 \text{ GeV}) = 0.496 \text{ MeV} ,$$
$$m_\mu(1 \text{ GeV}) = 104.57 \text{ MeV} , \qquad (2.74)$$
$$m_\tau(1 \text{ GeV}) = 1.7835 \text{ GeV} .$$

G. Higgs-boson and top-quark masses

The Higgs-boson and top-quark masses have not been measured directly at present; however, their values af-

fect radiative corrections such as Δr. Consistency with experimental data on $\sin^2 \theta_W$ requires $M_t < 197$ GeV for $M_H = 1$ TeV at 99% C.L. assuming no physics beyond the standard model [44]. Precision measurements of the Z mass and its decay properties combined with low-energy neutral-current data have been used to set stringent bounds on the top-quark mass within the minimal standard model. A global analysis of this data yields $M_t = 122^{+41}_{-32}$ GeV, for all allowed values of M_H [45]. Recent direct search results set the experimental lower bound $M_t \gtrsim 91$ GeV. As for the Higgs boson, the analysis of Ref. [45] gives the restrictive bound, $M_H \lesssim 600$ GeV, if $M_t < 120$ GeV, and $M_H < 6$ TeV, for all allowed M_t. Since perturbation theory breaks down for $M_H \gtrsim 1$ TeV, the latter bound on the Higgs-boson mass is not necessarily meaningful. LEP data set a lower bound on the Higgs-boson mass of 48 GeV [46].

In our analysis, initial values of the $\overline{\text{MS}}$ running top-quark mass m_t and of the scalar quartic coupling λ at M_Z are chosen arbitrarily (consistent with the bounds quoted above). As noted earlier in Sec. II A, these running parameters are not equal to their physical counterparts. However, any reasonable prediction for the masses of the top quark and of the Higgs boson that may come from our analysis should be that of experimentally relevant, physical masses. Therefore, formulas similar to Eq. (2.73) relating $\overline{\text{MS}}$ running parameters to physical masses are needed. To calculate the physical or pole mass of the top quark, we use Eq. (2.65) in its general form

$$\frac{M_t}{m_t(M_t)} = 1 + \frac{4}{3} \frac{\alpha_s(M_t)}{\pi}$$
$$+ \left[16.11 - 1.04 \sum_{i=1}^{5} \left(1 - \frac{M_i}{M_t} \right) \right]$$
$$\times \left(\frac{\alpha_s(M_t)}{\pi} \right)^2 , \qquad (2.75)$$

where M_i, $i = 1, \ldots, 5$, represent the masses of the five lighter quarks. Likewise the physical mass of the Higgs boson can be extracted from the relation [47]

$$\lambda(\mu) = \frac{G_\mu}{\sqrt{2}} M_H^2 [1 + \delta(\mu)] , \qquad (2.76)$$

where $\delta(\mu)$ contains the radiative corrections. Its form is rather elaborate and we relegate it to Appendix B. Equations (2.75) and (2.76) are highly nonlinear functions of M_t and M_H, respectively. Their solution requires numerical routines that are described in Appendix C.

H. Vacuum expectation value of the scalar field

A value for the vacuum expectation value (VEV) of the scalar field may be extracted from the well-known lowest order relation

$$v = (\sqrt{2} G_\mu)^{-\frac{1}{2}} = 246.22 \text{ GeV} . \qquad (2.77)$$

From the very well-measured value of the muon lifetime, $\tau_\mu = 2.197\,035 \pm 0.000\,040 \times 10^{-6}$ s [24], the Fermi constant can be extracted using the formula [48]
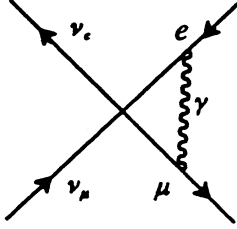
FIG. 1. Electromagnetic correction to muon decay.

$$\tau_\mu^{-1} = \frac{G_\mu^2 m_\mu^5}{192\pi^3} f\left(\frac{m_e^2}{m_\mu^2}\right)\left(1 + \frac{3}{5}\frac{m_\mu^2}{m_W^2}\right)$$
$$\times \left[1 + \frac{\alpha(m_\mu)}{2\pi}\left(\frac{25}{4} - \pi^2\right)\right], \qquad (2.78)$$

where

$$f(x) = 1 - 8x + 8x^3 - x^4 - 12x^2 \ln x , \qquad (2.79)$$

giving

$$G_\mu = 1.166\,37 \pm 0.000\,02 \times 10^{-5} \text{ GeV}^{-2} . \qquad (2.80)$$

This parameter may be viewed as the coefficient of the effective four-fermion operator for muon decay in an effective low-energy theory:

$$\frac{G_\mu}{\sqrt{2}}[\overline{\nu}_e\gamma^\beta(1-\gamma_5)e][\overline{\mu}\gamma_\beta(1-\gamma_5)\nu_\mu] . \qquad (2.81)$$

A direct calculation (e.g., in the Landau gauge) of the electromagnetic corrections (see Fig. 1) yields that the operator is finitely renormalized (i.e., G_μ does not run) [19, 49]. Another way to see this is by using a Fierz transformation to rewrite the above expression:

$$\frac{G_\mu}{\sqrt{2}}[\overline{\nu}_e\gamma^\beta(1-\gamma_5)\nu_\mu][\overline{\mu}\gamma_\beta(1-\gamma_5)e] . \qquad (2.82)$$

The neutrino current does not couple to the photon field, and the $e - \mu$ current is conserved and is hence not multiplicatively renormalized.

We need an initial value for the running vacuum expectation value at some scale μ. Wheater and Llewellyn Smith [50] consider muon decay to order α in the context of the full electroweak theory and derive an equation relating a $\overline{\text{MS}}$ running G_μ to the experimentally measured value. From this formula we can extract a value for $v(M_Z)$. However, this formula is derived in the 't Hooft–Feynman gauge, and the evolution equation (A18) of Appendix A for the VEV is valid only in the Landau gauge. Nevertheless, motivated by the discussion of the previous paragraph, we choose the initial condition for the VEV to be $v(M_W) = 246.22$ GeV. Using the initialization algorithm (see Appendix C), we arrive at $v(M_Z)$. We find that this procedure leads to no significant correction, and we therefore take, *ab initio*, $v(M_Z) = 246.22$ GeV.

III. THRESHOLD ANALYSIS

A. Effective gauge theories

We are using the $\overline{\text{MS}}$ renormalization scheme to determine the running of the standard model couplings. From the Appelquist-Carrazzone decoupling theorem [51] we expect the physics at energies below a given mass scale to be independent of the particles with masses higher than this threshold. However, such minimal subtraction schemes are not physical in the sense that they are scale dependent and mass independent so that the decoupling theorem is not manifest. As described in Refs. [11, 12], we have to formulate a low-energy effective theory by integrating out the heavy fields to one loop and find matching functions in order to take care of the threshold effects. We give a brief review of threshold effects in the running of the gauge couplings for a spontaneously broken GUT and for the standard model. Details can be found in the appendices of Ref. [12]. We next discuss thresholds in running fermion masses, a subject which to our knowledge has not been adequately treated in the literature. In Sec. IV we give a quantitative description of the effect of thresholds in the running parameters.

The starting point for treating thresholds in MS and $\overline{\text{MS}}$ schemes is the construction of low-energy effective gauge theories [11–13]. The basic idea is to integrate out the heavy fields in such a way that the remaining effective action is gauge invariant under the residual gauge group. Let the simple gauge group G be broken to $\tilde{G}$, and let Φ and ϕ be a set of heavy and light fields, respectively. Then the action $\tilde{I}[\phi]$ of the effective field theory is obtained from the action $I[\phi, \Phi]$ of the full theory by functional integration over the heavy fields:

$$e^{i\tilde{I}[\phi]} = \int [d\Phi]e^{iI[\phi,\Phi]} . \qquad (3.1)$$

Because there are no superheavy fields in the effective theory the decoupling theorem is not needed. However, there is a difficulty having to do with gauge invariance. Namely, in order to integrate out the heavy fields one has to add a gauge fixing term, and such a term usually spoils the gauge invariance of the low-energy theory. The usual R_ξ gauge fixing action for the full gauge group is

$$I_{\text{GF}} = -\frac{1}{2}\sum_\alpha \int d^4x \, f_\alpha^2(x;\phi,\Phi) , \qquad (3.2)$$

where, for example,

$$f_\alpha = \xi^{-1/2}[\partial_\mu A_\alpha^\mu + ig\xi vt_{\alpha S}S] , \qquad (3.3)$$

where α runs over all generators $t_{\alpha S}$ of G, A_α^μ are the gauge fields, and S is a column of Hermitian scalar fields with vacuum expectation value v. However, when the heavy gauge fields are integrated out with the natural choice of the gauge fixing functional as in Eq. (3.3) but summed only over the index of the broken group generators (given in uppercase Latin letters), one obtains an effective theory that is not invariant under $\tilde{G}$. We correct this by changing the derivative in Eq. (3.3) into a $\tilde{G}$

covariant derivative so that f becomes

$$f_A = \xi^{-1/2}[\partial_\mu A_A^\mu + g C_{ABa} A_B^\mu A_{a\mu} + ig\xi vt_{AS}S] \;,$$

(3.4)

where the lower-case Latin indices run over the generators of the unbroken gauge group and $C_{\alpha\beta\gamma}$ are the com-

pletely antisymmetrized structure constants of G.

Applying this gauge fixing to the breakdown of G into a direct product of simple or Abelian groups $\tilde{G}_i$, Refs. [11, 12] state the result of integrating out all heavy fields to one loop for the case $\xi = 1$. The running gauge coupling constants of the effective theory are related to that of the full theory by [11, 12]

$$g_i(\mu) = g(\mu) + \frac{g(\mu)^3}{96\pi^2}\left\{ \mathrm{Tr}\left[t_{iS}^2 \Lambda \ln\left(\frac{M_S}{\mu}\right)\right] + 8\,\mathrm{Tr}\left[t_{iF}^2 \ln\left(\frac{\sqrt{2}M_F}{\mu}\right)\right] + \mathrm{Tr}\,t_{iV}^2 - 21\,\mathrm{Tr}\left[t_{iV}^2 \ln\left(\frac{M_V}{\mu}\right)\right]\right\}\;,$$

(3.5)

where Λ projects onto non-Nambu-Goldstone boson scalar fields, t_{iS}, t_{iF}, and t_{iV} are the representation matrices of $\tilde{G}_i$ for the heavy scalar, fermion, and vector fields, respectively. $M_{S,F,V}$ are their mass matrices. This formula can also be used to determine the effect of integrating out a heavy quark in lower-energy QCD. Here one need only include the heavy fermion part of the integration to determine the low-energy gauge coupling in terms of the coupling of the full theory above the heavy quark threshold. Note that Eq. (3.5) only holds in the neighborhood of $\mu \sim M$, M being the heavy scale, and as such provides an initial condition for the running of the effective couplings for $\mu \ll M$.

In application to the standard model we will integrate out the heavy fields using matching functions as described above. As we are running couplings to two loops, it is sufficient to integrate out these fields to one loop. The heavy gauge bosons, their ghosts, and the top quark are integrated out near M_W, the other fermions at their physical masses M_f. One may integrate out different mass particles at one scale as long as the two-loop contribution to coupling constant renormalization between two threshold scales is negligible. The errors arising from not integrating out fields at a scale μ exactly equal to their physical mass M is of order $\alpha_{1,2,3} \ln(M/\mu)$, which is negligible within the perturbative regime.

B. Gauge coupling thresholds

At the electroweak threshold, the point at which W and Z bosons, their associated Nambu-Goldstone bosons, ghosts, and the top quark are integrated out, one imposes matching conditions similar to Eq. (3.5). Above the threshold the theory has the $SU(3)_C \times SU(2)_L \times U(1)_Y$ gauge symmetry of the standard model and a $SU(3)_C \times U(1)_{\mathrm{em}}$ effective symmetry below. Following Refs. [11, 12], we gauge fix the standard model in such a way that the low-energy theory is $SU(3)_C \times U(1)_{\mathrm{em}}$ invariant after the SU(2) gauge fields are integrated out. The gauge fixing part of the Lagrangian is

$$\mathcal{L}_{\mathrm{GF}} = -\frac{1}{2\xi}\{ [\partial_\mu W_1^\mu + ig_2\xi v_i(\tau_1)_{ij}\phi_j + g_2 s W_2^\mu A_\mu]^2$$

$$+ [\partial_\mu W_2^\mu + ig_2\xi v_i(\tau_2)_{ij}\phi_j + g_2 s W_1^\mu A_\mu]^2$$

$$+ [\partial_\mu Z^\mu + ig_2 c^{-1} v_i(\tau_3)_{ij}\phi_j]^2 \}\;,$$

(3.6)

where $c = \cos\theta_W$, $s = \sin\theta_W$, and ϕ_i is the shifted Higgs field with v_i its vacuum expectation value. The heavy gauge bosons, Higgs and Nambu-Goldstone bosons, and ghosts are integrated out to one loop by evaluating their contribution to photon vacuum polarization. The result is [12]

$$\frac{1}{\alpha(\mu)} = \frac{1}{\alpha_2(\mu)s^2(\mu)} - 4\pi\Omega(\mu)\;,$$

(3.7)

where

$$\Omega(\mu) = \frac{2}{48\pi^2}\left[1 - 21\ln\left(\frac{M_W}{\mu}\right)\right]\;,$$

(3.8)

and where $s(\mu)$ is defined in Eq. (2.4). Using the GUT normalization for α_1, one can also write

$$\frac{1}{\alpha_1} = \frac{3}{5}\left[\frac{1 - s^2(\mu)}{\alpha(\mu)}\right] + \frac{3}{5}[1 - s^2(\mu)]4\pi\Omega(\mu)\;,$$

$$\frac{1}{\alpha_2} = \frac{s^2(\mu)}{\alpha(\mu)} + 4\pi\Omega(\mu)s^2(\mu)\;,$$

(3.9)

where the first term on the right side of each equation gives the usual tree-level relation. One can always impose these tree-level relations by fixing μ so that the matching function Ω vanishes. Here this occurs for $\bar{\mu} = 0.95 M_W$.

When the heavy top quark is included in the analysis one may integrate it out separately in which case one has an effective standard model without a top quark between M_W and M_t. Alternatively one can integrate it out at the same scale as the massive gauge bosons in which case the top-quark loop in the photon propagator contributes to the matching function above

$$\Omega(\mu) \to \Omega(\mu) + 2b_{\mathrm{QED}}^{(t)} \ln\left(\frac{M_t}{\mu}\right)\;,$$

(3.10)

where $b_{\mathrm{QED}}^{(t)} = 1/9\pi^2$ is the contribution of the top quark to the coefficient of e^3 in the QED β function. The perturbativity of QED at M_W and the small mass difference between the top quark and gauge bosons [so that $\alpha \ln(M_t/M_W)$ is small] means that this is a reliable approximation. We incorporate this matching condition which includes the top quark into our numerical integration of the electroweak β functions.

The strong QCD coupling has thresholds near quark masses. The effect of integrating out a quark is to pro-

duce a matching condition of the form

$$\frac{1}{\alpha_s(\mu)} = \frac{1}{\alpha_3(\mu)} - 4\pi\Omega_3(\mu) \ , \tag{3.11}$$

where

$$\Omega_3(\mu) = 2b_3^{(q)}\ln\left(\frac{M_t}{\mu}\right) \ , \tag{3.12}$$

and $b_3^{(q)} = 1/24\pi^2$ appears as the contribution of each quark to the one-loop QCD β function: $\beta_{g_3} = b_3 g_3^3$. The top quark is integrated out at $\mu = \overline{\mu}$ so that the strong coupling does not match continuously across the threshold. For the other heavy quark thresholds, however, we choose the renormalization scale for matching to be the physical quark masses so that the matching functions vanish there. The only effect of these thresholds is a step in the number of flavors n_{fl} as each quark threshold is passed [52].

Likewise the QED coupling in the low-energy theory has thresholds at charged particle masses, the matching condition having the form

$$\frac{1}{\alpha_{em}} = \frac{1}{\alpha(\mu)} - 4\pi\Omega_{QED}(\mu) \ . \tag{3.13}$$

Here α_{em} is evaluated in the zero frequency limit and

$$\Omega_{QED}(\mu) = \frac{1}{48\pi^2}\left[8\sum_F Q_F^2\ln\left(\frac{M_F}{\mu}\right) \right.$$
$$\left. + \sum_S Q_S^2\ln\left(\frac{M_S}{\mu}\right) \right] \ . \tag{3.14}$$

The F and S subscripts refer to charged fermions and scalars, respectively. Again the matching function vanishes at each particle mass so the effect of the threshold is simply to produce a step in the number of fermions or scalars of a given charge.

C. Threshold effects in fermion masses (Yukawas)

It is important to realize that the running fermion masses also experience threshold effects near physical particle masses. To our knowledge there is no mention

of these effects in the literature although they are potentially important in analyses of mass relations predicted in many grand unified models and in the full two-loop running of gauge couplings. Since the Higgs field is integrated out at the electroweak scale the Yukawa couplings appear in the low-energy theory through particle masses and various nonrenormalizable (NR) interactions:

$$\mathcal{L}_{SM} = -y_{ij}^a v_a\overline{\psi}_i\psi_j - y_{ij}^a\phi_a\overline{\psi}_i\psi_j + \cdots \ ,$$
$$\mathcal{L}_{low} = -m_{ij}\overline{\psi}_i\psi_j + \text{NR terms} + \cdots \ . \tag{3.15}$$

We evaluate the matching conditions in $\overline{\text{MS}}$, running fermion masses at the electroweak threshold by integrating out Higgs, Nambu-Goldstone, and gauge bosons as well as ghosts and the top quark. (The Higgs field does not contribute at one loop to these matching functions as it has no $SU(3)_C \times U(1)_{em}$ couplings.)

The diagrams corresponding to integrating out these fields that contribute to one-loop renormalization of quark and lepton two-point Green's functions in the standard model are depicted in Fig. 2. As in Eq. (3.6), we work in a specific gauge required for gauge invariance of the low-energy effective Lagrangian under $SU(3)_C \times U(1)_{em}$. As for the gauge bosons the finite piece of the contributions of these diagrams gives the matching function and the divergent piece gives the one-loop β function (see Appendix A). In terms of bare parameters and fields the relevant parts of the standard model Lagrangian for this calculation are

$$\mathcal{L}_{SM} = \overline{\psi}_{iL}i\!\!\not{D}\psi_{iL} + \overline{\psi}_{iR}i\!\!\not{D}\psi_{iR}$$
$$-y_{ij}^a v_a\overline{\psi}_{iL}\psi_{jR} - y_{ij}^a\phi_a\overline{\psi}_{iL}\psi_{jR} + \text{H.c.} + \cdots \ , \tag{3.16}$$

where ψ_i can be a quark or lepton and i is a family index. When the heavy fields are integrated out we generate the low-energy effective Lagrangian

$$\mathcal{L}_{low} = (1 + K_{iL})\overline{\psi}_{iL}i\!\!\not{D}\psi_{iL} + (1 + K_{iR})\overline{\psi}_{iR}i\!\!\not{D}\psi_{iR}$$
$$-(m_{ij} + \delta m_{ij})(\overline{\psi}_{iL}\psi_{jR} + \text{H.c.}) + \cdots \ , \tag{3.17}$$

where $m_{ij} = y_{ij}^a v_a$. The $K_{L,R}$'s contain wave function renormalization contributions of the left- and right-
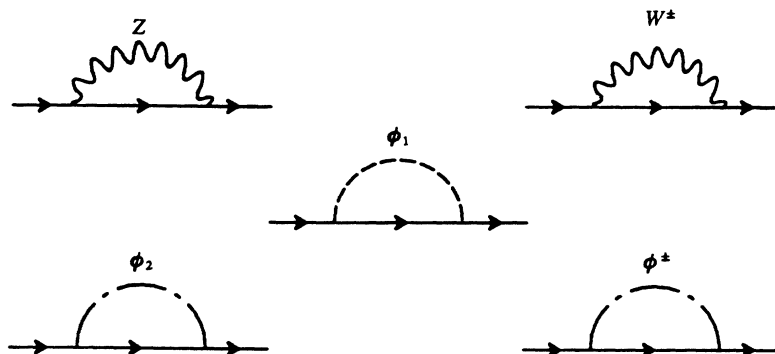

FIG. 2. One-loop corrections to fermion two-point functions.

handed fermion fields along with finite parts, and δm_{ij} is the fermion self-energy contribution.

We must rescale the bare fermion fields in the low-energy theory so they have the canonically normalized kinetic term:

$$\psi'_{iL,R} = (1 + K_{iL,R})^{1/2}\psi_{iL,R} .\tag{3.18}$$

The relation between the standard model and low-energy bare masses becomes

$$m_{ij}^{(\text{low})} = (m_{ij}^{(\text{SM})} + \delta m_{ij})(1 + K_{iL})^{-1/2}(1 + K_{jR})^{-1/2} .\tag{3.19}$$

Note that the left- and right-handed fermion fields are renormalized differently due to their different gauge couplings, so $K_L \neq K_R$. Also note that in the case of quarks the self-energy corrections δm_{ij} introduce additional non-diagonal contributions to the mass matrix. However, in the limit $M_q \ll M_W$ these nondiagonal contributions are negligible.

We determine the matching functions for the fermion masses in the standard model in terms of their electroweak quantum numbers. Since we work in the limit where the self-energy contributions are diagonal, we write $\delta m_{ij} = \delta_{ij}m_i(1 + K_{im})$. The functions K_{iL}, K_{iR}, and K_{im} are

$$K_{iL} = \frac{g_2^2}{256\pi^2 c^2}\left(\frac{\kappa_L^{i\prime}}{\eta} - \kappa_L^i\right) ,$$

$$K_{iR} = \frac{g_2^2}{256\pi^2 c^2}\left(\frac{\kappa_R^{i\prime}}{\eta} - \kappa_R^i\right) ,\tag{3.20}$$

$$K_{im} = \left(\frac{g_2^2}{64\pi^2 c^2}\right)\left(\frac{\kappa_m^{i\prime}}{\eta} - \kappa_m^i\right) ,$$

where

$$\frac{1}{\eta} = \frac{1}{\epsilon} + \ln 4\pi - \gamma_E .\tag{3.21}$$

We work in the $\xi = 1$ gauge. The coefficients of the divergent parts

$$\kappa_L^{i\prime} = (g_V^i + g_A^i)^2 + 8c^2 ,$$

$$\kappa_R^{i\prime} = (g_V^i - g_A^i)^2 ,\tag{3.22}$$

$$\kappa_m^{i\prime} = g_V^{i2} - g_A^{i2} ,$$

give the one-loop β functions. Those of the finite parts,

$$\kappa_L^i = (g_V^i + g_A^i)^2\left(\ln\frac{M_Z^2}{\mu^2} - \frac{1}{2}\right) + 8c^2\left(\ln\frac{M_W^2}{\mu^2} - \frac{1}{2}\right) ,$$

$$\kappa_R^i = (g_V^i - g_A^i)^2\left(\ln\frac{M_Z^2}{\mu^2} - \frac{1}{2}\right) ,\tag{3.23}$$

$$\kappa_m^i = (g_V^{i2} - g_A^{i2})\left(\ln\frac{M_Z^2}{\mu^2} - \frac{1}{2}\right) ,$$

give the matching functions. Here $g_{V,A}^i = 2(g_L^i \pm g_R^i)$, where $g_{L,R}^i = T_3{}^i{}_{L,R} - s^2 Q^i$ and $T_3{}^i{}_{L,R}$ and Q^i are the third components of weak isospin and the electric charge, respectively, for a given handedness of the ith fermion. For the different quark and lepton charge sectors one has

$$\begin{aligned}
g_A^\nu &= +1, & g_V^\nu &= +1, \\
g_A^e &= -1, & g_V^e &= -1 + 4s^2, \\
g_A^u &= +1, & g_V^u &= +1 - \tfrac{8}{3}s^2, \\
g_A^d &= -1, & g_V^d &= -1 + \tfrac{4}{3}s^2 .
\end{aligned}\tag{3.24}$$

Inserting the β functions into Eq. (3.19) we obtain the relation between the diagonalized, renormalized masses in the standard model and the low-energy effective theory:

$$m_i^{(\text{low})}(\mu) = m_i^{(\text{SM})}(\mu)\left\{1 + \frac{g_2^2}{64\pi^2 c^2}\left[\kappa_m^i(\mu) + \frac{1}{8}(\kappa_L^i + \kappa_R^i)\right]\right\} .\tag{3.25}$$

IV. QUANTITATIVE ANALYSIS

We depict the results of numerically integrating the β functions for the standard model parameters from 1 GeV to Planck mass in Figs. 3 to 11. For most of these plots, we have made the arbitrary choice, $M_t = M_H = 100$ GeV. In some figures, we superimpose one- and two-loop evolution. For example, in Fig. 3 we display the evolution of the inverse of each of the three gauge couplings. In it, we see the "GUT triangle" signifying the absence of grand unification, assuming the standard model as an effective theory in the desert up to the Planck scale. Here, the differences between one- and two-loop evolutions appear in the high-energy regime. Differences are also manifest for the strong coupling at low energies where it becomes large. In Fig. 4 we display these same inverse couplings, but this time we include the associated uncertainties in their values. We note, as is well known, that the uncertainties do not fill in the "GUT triangle." Figures 5, 6, and 7 are similar to Fig. 3 except they display the evolution of the light mass fermions (m_e, m_u, and m_d), the intermediate mass fermions (m_μ and m_s), and the heavy mass fermions (m_τ, m_c, and m_b), respectively. We conclude that the largest differences between
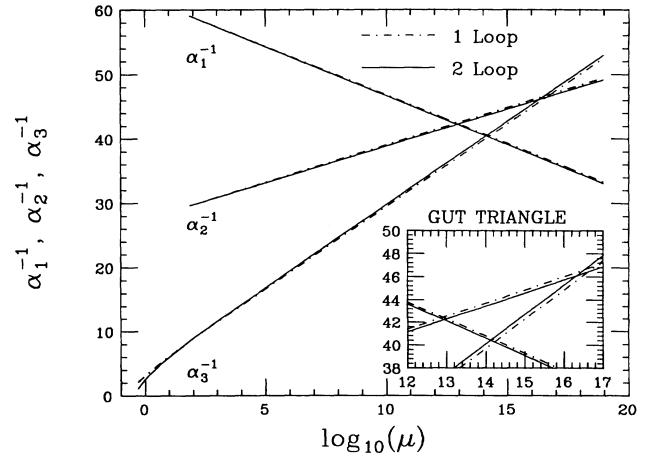

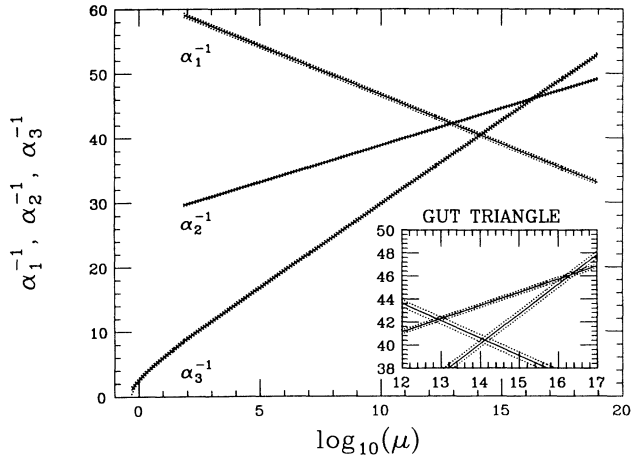FIG. 3. Running of the inverse gauge couplings using their central value as initial data.

FIG. 4.　Running of the inverse gauge couplings using their propagated experimental errors for the two-loop case only.
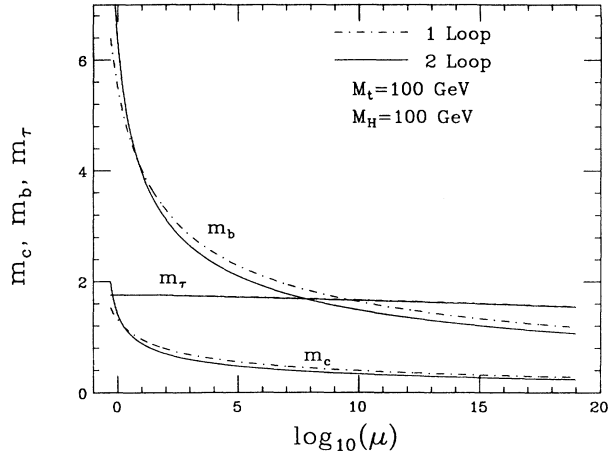
FIG. 7.　Heavy quark and lepton masses for $M_t = 100$ GeV and $M_H = 100$ GeV.
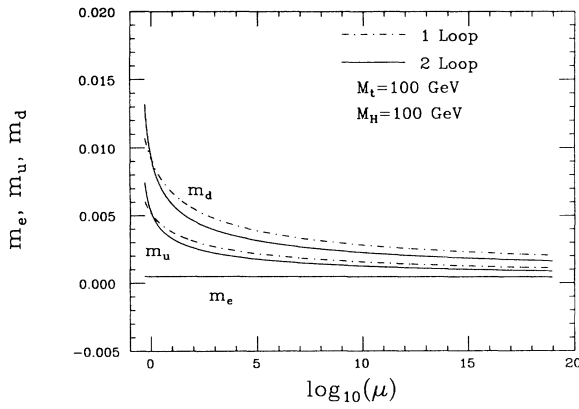
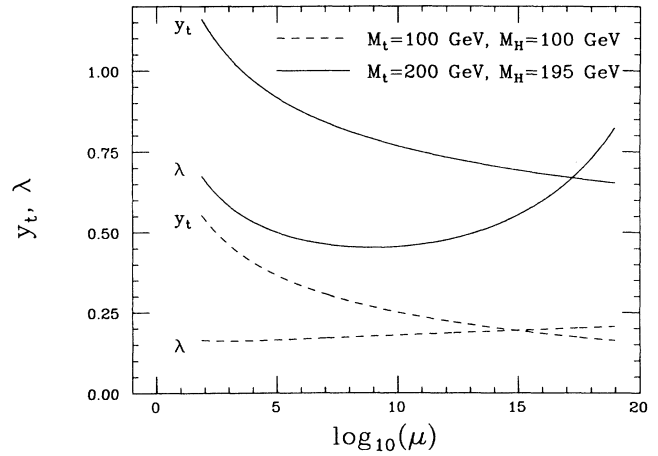FIG. 5.　Light quark and lepton masses for $M_t = 100$ GeV and $M_H = 100$ GeV.

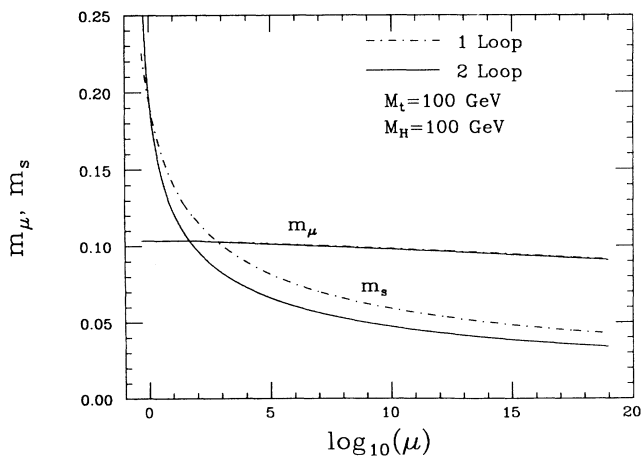FIG. 8.　Top Yukawa and scalar quartic couplings.

FIG. 6.　Intermediate quark and lepton masses for $M_t = 100$ GeV and $M_H = 100$ GeV.
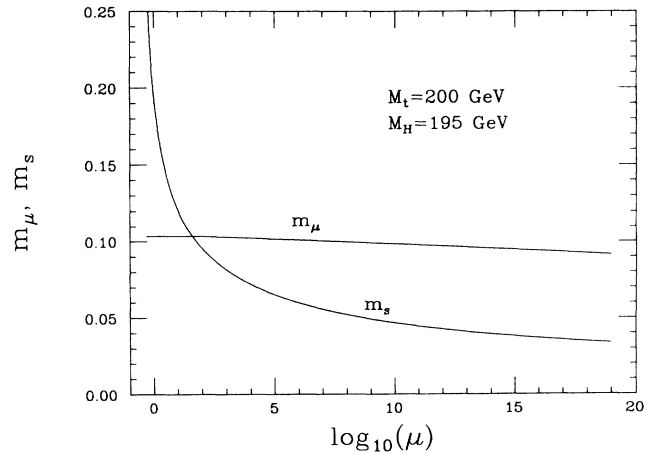
FIG. 9.　Intermediate quark and lepton masses for $M_t = 200$ GeV and $M_H = 195$ GeV.
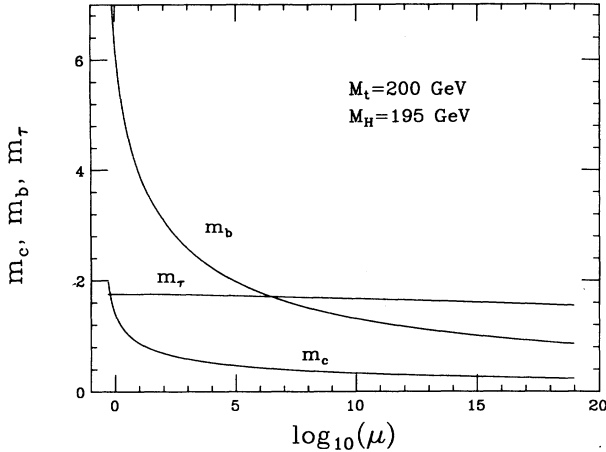
FIG. 10. Heavy quark and lepton masses for $M_t = 200$ GeV and $M_H = 195$ GeV.
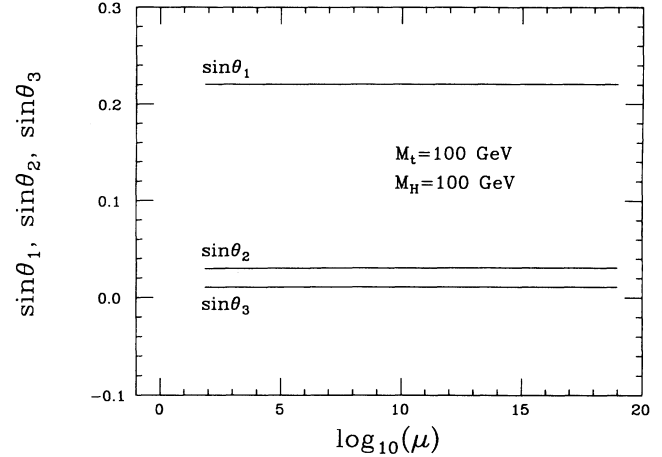

FIG. 11. CKM mixing angles for $M_t = 100$ GeV and $M_H = 100$ GeV.

one-loop versus two-loop evolution occur in the bottom, charm, and strange quark masses in these cases. In Fig. 8, we plot the quartic coupling λ and the top Yukawa coupling y_t for $(M_t = 100$ GeV, $M_H = 100$ GeV) and for $(M_t = 200$ GeV, $M_H = 195$ GeV). These two couplings are the only unknown parameters of the standard model. We have studied the effects of changing the values of M_t and M_H in our analyses of the running of the other parameters. We observed that, for any M_t between 100 GeV and 200 GeV, varying M_H, while maintaining perturbativity and vacuum stability, did not affect appreciably the evolution of any of the other parameters. However, changing M_t itself showed a significant difference in the running of the heavier quarks. To illustrate this, in Figs. 9 and 10 we display plots similar to Figs. 6 and 7 but for $M_t = 200$ GeV and $M_H = 195$ GeV. In particular, in Fig. 10 we note that the intersection point between the bottom quark and the τ lepton moves down to a lower scale for this case of a higher top-quark mass. This is expected since from Eq. (A10) one can see that the bottom-type Yukawa couplings are driven down by an increased top Yukawa coupling. This is to be contrasted with the SUSY GUT case in which the bottom Yukawa β function is such that this crossing point is shifted toward a higher scale with an increased top mass. In an SU(5) SUSY GUT model, the equality of the bottom and τ Yukawa couplings at the scale of unification was used to get bounds on the top-quark and Higgs-boson masses [5]. Lastly, we display the running of the CKM angles in Fig. 11. We are using the initial data: $\sin\theta_1 = 0.2206$,

$\sin\theta_2 = 0.0298$, and $\sin\theta_3 = 0.0106$. Also we have taken $\delta = 90°$ which corresponds to the case of maximal CP violation. As mentioned in Sec. II D, the evolution curves for these angles are effectively flat.

In the present case of the standard model, we find that two-loop running of the parameters does at times improve on the one-loop running. Indeed, we have tabulated the differences of several parameters in their one- versus two-loop values at various scales for the cases $(M_t = 100$ GeV, $M_H = 100$ GeV) and $(M_t = 200$ GeV, $M_H = 195$ GeV). Table II illustrates the difference one-loop versus two-loop running makes in the ratio m_b/m_τ, for the three scales 10^2 GeV, 10^4 GeV, and 10^{16} GeV.

Clearly, the difference between one- and two-loop results is more pronounced at higher scales, as expected. Over all these scales the difference is never less than 5.5%. We note that the ratio becomes equal to one well below the scale of grand unification as noted in the discussion of Figs. 7 and 10. Table III presents a similar comparison for the top Yukawa coupling. Here, two loops represent a smaller correction with the difference at all scales always being less than 5%.

Finally, Table IV displays the same analysis for α_s for the case $M_t = M_H = 100$ GeV. We observe no appreciable deviation from the tabulated values for any $M_t \lesssim 200$ GeV (except in the low-energy regime where the difference is at most $\sim 4\%$).

At scales $\lesssim M_Z$, the inclusion of two loops is important in the evolution of the strong coupling (and of the quark masses). Indeed, we find that the pure QCD three-loop

TABLE II. Difference between one- and two-loop running in m_b/m_τ.

| | $M_t = 100$ GeV | | | $M_t = 200$ GeV | | |
	10^2 GeV	10^4 GeV	10^{16} GeV	10^2 GeV	10^4 GeV	10^{16} GeV
One loop	1.938	1.499	0.8326	1.868	1.392	0.6647
Two loop	1.937	1.463	0.7962	1.769	1.285	0.6047

TABLE III. A similar comparison as in Table II for y_t.

	$M_t = 100$ GeV			$M_t = 200$ GeV		
	10^2 GeV	10^4 GeV	10^{16} GeV	10^2 GeV	10^4 GeV	10^{16} GeV
One loop	0.7879	0.6076	0.2830	1.133	0.9780	0.7145
Two loop	0.7873	0.5940	0.2701	1.143	0.9700	0.6816

contribution is also significant and therefore include it in the running of the strong coupling and of the quark masses in the low-energy region. As seen in this table, the combined two and three loops in the low-energy regime account for a 17% difference at 1 GeV in α_s.

Although in the cases considered in these last two tables there does not appear to be a significant difference in two-loop over one-loop evolution at scales above M_Z, the first table does show a 10% difference at the scale, 10^{16} GeV. We expect two-loop effects to be more important when the theory is extended, e.g., to include supersymmetry and/or grand unification.

The effects of using a naive step approximation versus a proper treatment of thresholds are numerically unimportant for the cases discussed above. Indeed they are less important than the two-loop effects. We note, however, that the inclusion of non-naive threshold effects is significant in the numerical analysis of extensions of the standard model.

V. CONCLUSION

In the present paper we have collected the necessary tools for renormalization-group analyses of the standard model. We worked in the $\overline{\text{MS}}$ renormalization scheme using the standard model two-loop renormalization-group β functions. We evolved the parameters of the standard model, i.e., the gauge couplings, the quark and lepton masses, the Yukawa sector mixing angles and phase, and the scalar quartic coupling from a mass scale of 1 GeV to Planck mass. We reviewed the extraction from experiment of the initial values for these parameters with specific emphasis on the extraction of the strong coupling constant and of the quark masses (especially those of the charm and bottom flavor). We endeavored to treat the threshold effects appropriately, i.e., rather than using naive step function implementation of thresholds, we implemented one-loop matching conditions for both gauge boson and fermion mass thresholds. We found that in the case of the standard model these matching conditions did not improve essentially upon the simple use of step functions. Indeed, two loops versus one loop represented a more significant effect, albeit sometimes small. For com-

pleteness, we included plots exhibiting these different features for all the parameters of the standard model.

The raison d'être of this study is to present a template for future investigations. We can now add the effects of extensions of the standard model and study their consequences. This program has already been carried out in some special cases involving supersymmetry for the gauge couplings [4] and for the Yukawa couplings [5, 6] with interesting consequences.

APPENDIX A: STANDARD MODEL β FUNCTIONS

In this appendix we compile the renormalization-group β functions of the standard model. These have appeared in one form or another in various sources. We have endeavored to confirm their validity through a comparative analysis of the literature. Our main source is Ref. [7]. Following their conventions,

$$\mathcal{L} = \overline{Q}_L \tilde{\Phi} \mathbf{Y}_u{}^\dagger u_R + \overline{Q}_L \Phi \mathbf{Y}_d{}^\dagger d_R + \overline{\ell}_L \Phi \mathbf{Y}_e{}^\dagger e_R + \text{H.c.}$$
$$- \frac{1}{2}\lambda (\Phi^\dagger \Phi)^2 , \tag{A1}$$

where flavor indices have been suppressed, and where Q_L and ℓ_L are the quark and lepton SU(2) doublets, respectively,

$$Q_L = \begin{pmatrix} u_L \\ d_L \end{pmatrix} , \quad \ell_L = \begin{pmatrix} \nu_L \\ e_L \end{pmatrix} . \tag{A2}$$

Φ and $\tilde{\Phi}$ are the Higgs scalar doublet and its SU(2) conjugate:

$$\Phi = \begin{pmatrix} \phi^+ \\ \phi^0 \end{pmatrix} , \quad \tilde{\Phi} = i\tau_2 \Phi . \tag{A3}$$

u_R, d_R, and e_R are the quark and lepton SU(2) singlets, and $\mathbf{Y}_{u,d,e}$ are the matrices of the up-type, down-type, and lepton-type Yukawa couplings.

The β functions for the gauge couplings are

TABLE IV. Same analysis as in Table II for α_s.

	1 GeV	10^2 GeV	10^4 GeV	10^{16} GeV
One loop	0.3128	0.1118	0.07103	0.02229
Two and three loop	0.3788	0.1117	0.07039	0.02208

$$\frac{dg_l}{dt} = -b_l\frac{g_l^3}{16\pi^2} - \sum_k b_{kl}\frac{g_k^2 g_l^3}{(16\pi^2)^2} - \frac{g_l^3}{(16\pi^2)^2}\text{Tr}\{C_{lu}\mathbf{Y}_u{}^\dagger\mathbf{Y}_u + C_{ld}\mathbf{Y}_d{}^\dagger\mathbf{Y}_d + C_{le}\mathbf{Y}_e{}^\dagger\mathbf{Y}_e\}\ ,\tag{A4}$$

where $t = \ln\mu$ and $l = 1, 2, 3$, corresponding to the gauge group $\text{SU}(3)_C \times \text{SU}(2)_L \times \text{U}(1)_Y$ of the standard model. The various coefficients are defined to be

$$\begin{aligned}
b_1 &= -\frac{4}{3}n_g - \frac{1}{10}\ , \\
b_2 &= \frac{22}{3} - \frac{4}{3}n_g - \frac{1}{6}\ , \\
b_3 &= 11 - \frac{4}{3}n_g\ ,
\end{aligned}\tag{A5}$$

$$(b_{kl}) = \begin{pmatrix} 0 & 0 & 0 \\ 0 & \frac{136}{3} & 0 \\ 0 & 0 & 102 \end{pmatrix} - n_g\begin{pmatrix} \frac{19}{15} & \frac{1}{5} & \frac{11}{30} \\ \frac{3}{5} & \frac{49}{3} & \frac{3}{2} \\ \frac{44}{15} & 4 & \frac{76}{3} \end{pmatrix} - \begin{pmatrix} \frac{9}{50} & \frac{3}{10} & 0 \\ \frac{9}{10} & \frac{13}{6} & 0 \\ 0 & 0 & 0 \end{pmatrix}\ ,\tag{A6}$$

and

$$(C_{lf}) = \begin{pmatrix} \frac{17}{10} & \frac{1}{2} & \frac{3}{2} \\ \frac{3}{2} & \frac{3}{2} & \frac{1}{2} \\ 2 & 2 & 0 \end{pmatrix}\quad \text{with } f = u, d, e,\tag{A7}$$

with $n_g = \frac{1}{2}n_{\text{fl}}$.

In the Yukawa sector the β functions are

$$\frac{d\mathbf{Y}_{u,d,e}}{dt} = \mathbf{Y}_{u,d,e}\left(\frac{1}{16\pi^2}\beta_{u,d,e}^{(1)} + \frac{1}{(16\pi^2)^2}\beta_{u,d,e}^{(2)}\right)\ ,\tag{A8}$$

where the one-loop contributions are given by

$$\begin{aligned}
\beta_u^{(1)} &= \frac{3}{2}(\mathbf{Y}_u{}^\dagger\mathbf{Y}_u - \mathbf{Y}_d{}^\dagger\mathbf{Y}_d) + Y_2(S) - \left(\frac{17}{20}g_1^2 + \frac{9}{4}g_2^2 + 8g_3^2\right)\ , \\
\beta_d^{(1)} &= \frac{3}{2}(\mathbf{Y}_d{}^\dagger\mathbf{Y}_d - \mathbf{Y}_u{}^\dagger\mathbf{Y}_u) + Y_2(S) - \left(\frac{1}{4}g_1^2 + \frac{9}{4}g_2^2 + 8g_3^2\right)\ , \\
\beta_e^{(1)} &= \frac{3}{2}\mathbf{Y}_e{}^\dagger\mathbf{Y}_e + Y_2(S) - \frac{9}{4}(g_1^2 + g_2^2)\ ,
\end{aligned}\tag{A9}$$

with

$$Y_2(S) = \text{Tr}\{3\mathbf{Y}_u{}^\dagger\mathbf{Y}_u + 3\mathbf{Y}_d{}^\dagger\mathbf{Y}_d + \mathbf{Y}_e{}^\dagger\mathbf{Y}_e\}\ ,\tag{A10}$$

and the two-loop contributions are given by

$$\begin{aligned}
\beta_u^{(2)} =\ & \frac{3}{2}(\mathbf{Y}_u{}^\dagger\mathbf{Y}_u)^2 - \mathbf{Y}_u{}^\dagger\mathbf{Y}_u\mathbf{Y}_d{}^\dagger\mathbf{Y}_d - \frac{1}{4}\mathbf{Y}_d{}^\dagger\mathbf{Y}_d\mathbf{Y}_u{}^\dagger\mathbf{Y}_u + \frac{11}{4}(\mathbf{Y}_d{}^\dagger\mathbf{Y}_d)^2 + Y_2(S)\left(\frac{5}{4}\mathbf{Y}_d{}^\dagger\mathbf{Y}_d - \frac{9}{4}\mathbf{Y}_u{}^\dagger\mathbf{Y}_u\right) \\
& -\chi_4(S) + \frac{3}{2}\lambda^2 - 2\lambda(3\mathbf{Y}_u{}^\dagger\mathbf{Y}_u + \mathbf{Y}_d{}^\dagger\mathbf{Y}_d) + \left(\frac{223}{80}g_1^2 + \frac{135}{16}g_2^2 + 16g_3^2\right)\mathbf{Y}_u{}^\dagger\mathbf{Y}_u \\
& -\left(\frac{43}{80}g_1^2 - \frac{9}{16}g_2^2 + 16g_3^2\right)\mathbf{Y}_d{}^\dagger\mathbf{Y}_d + \frac{5}{2}Y_4(S) + \left(\frac{9}{200} + \frac{29}{45}n_g\right)g_1^4 \\
& -\frac{9}{20}g_1^2 g_2^2 + \frac{19}{15}g_1^2 g_3^2 - \left(\frac{35}{4} - n_g\right)g_2^4 + 9g_2^2 g_3^2 - \left(\frac{404}{3} - \frac{80}{9}n_g\right)g_3^4\ ,
\end{aligned}\tag{A11}$$

$$\begin{aligned}
\beta_d^{(2)} =\ & \frac{3}{2}(\mathbf{Y}_d{}^\dagger\mathbf{Y}_d)^2 - \mathbf{Y}_d{}^\dagger\mathbf{Y}_d\mathbf{Y}_u{}^\dagger\mathbf{Y}_u - \frac{1}{4}\mathbf{Y}_u{}^\dagger\mathbf{Y}_u\mathbf{Y}_d{}^\dagger\mathbf{Y}_d + \frac{11}{4}(\mathbf{Y}_u{}^\dagger\mathbf{Y}_u)^2 + Y_2(S)\left(\frac{5}{4}\mathbf{Y}_u{}^\dagger\mathbf{Y}_u - \frac{9}{4}\mathbf{Y}_d{}^\dagger\mathbf{Y}_d\right) \\
& -\chi_4(S) + \frac{3}{2}\lambda^2 - 2\lambda(3\mathbf{Y}_d{}^\dagger\mathbf{Y}_d + \mathbf{Y}_u{}^\dagger\mathbf{Y}_u) + \left(\frac{187}{80}g_1^2 + \frac{135}{16}g_2^2 + 16g_3^2\right)\mathbf{Y}_d{}^\dagger\mathbf{Y}_d \\
& -\left(\frac{79}{80}g_1^2 - \frac{9}{16}g_2^2 + 16g_3^2\right)\mathbf{Y}_u{}^\dagger\mathbf{Y}_u + \frac{5}{2}Y_4(S) - \left(\frac{29}{200} + \frac{1}{45}n_g\right)g_1^4
\end{aligned}$$

$$-\frac{27}{20}g_1^2 g_2^2 + \frac{31}{15}g_1^2 g_3^2 - \left(\frac{35}{4} - n_g\right)g_2^4 + 9g_2^2 g_3^2 - \left(\frac{404}{3} - \frac{80}{9}n_g\right)g_3^4,$$

$$\beta_e^{(2)} = \frac{3}{2}(\mathbf{Y}_e{}^\dagger \mathbf{Y}_e)^2 - \frac{9}{4}Y_2(S)\mathbf{Y}_e{}^\dagger \mathbf{Y}_e - \chi_4(S) + \frac{3}{2}\lambda^2 - 6\lambda \mathbf{Y}_e{}^\dagger \mathbf{Y}_e + \left(\frac{387}{80}g_1^2 + \frac{135}{15}g_2^2\right)\mathbf{Y}_e{}^\dagger \mathbf{Y}_e$$

$$+\frac{5}{2}Y_4(S) + \left(\frac{51}{200} + \frac{11}{5}n_g\right)g_1^4 + \frac{27}{20}g_1^2 g_2^2 - \left(\frac{35}{4} - n_g\right)g_2^4,$$

with

$$Y_4(S) = \left(\frac{17}{20}g_1^2 + \frac{9}{4}g_2^2 + 8g_3^2\right)\mathrm{Tr}\{\mathbf{Y}_u{}^\dagger \mathbf{Y}_u\} + \left(\frac{1}{4}g_1^2 + \frac{9}{4}g_2^2 + 8g_3^2\right)\mathrm{Tr}\{\mathbf{Y}_d{}^\dagger \mathbf{Y}_d\} + \frac{3}{4}(g_1^2 + g_2^2)\mathrm{Tr}\{\mathbf{Y}_e{}^\dagger \mathbf{Y}_e\}, \qquad \text{(A12)}$$

and

$$\chi_4(S) = \frac{9}{4}\mathrm{Tr}\left(3(\mathbf{Y}_u{}^\dagger \mathbf{Y}_u)^2 + 3(\mathbf{Y}_d{}^\dagger \mathbf{Y}_d)^2 + (\mathbf{Y}_e{}^\dagger \mathbf{Y}_e)^2 - \frac{2}{3}\mathbf{Y}_u{}^\dagger \mathbf{Y}_u \mathbf{Y}_d{}^\dagger \mathbf{Y}_d\right). \qquad \text{(A13)}$$

In the Higgs sector we present β functions for the quartic coupling and the vacuum expectation value of the scalar field. Here we correct a discrepancy in the one-loop contribution to the quartic coupling of Ref. [7]:

$$\frac{d\lambda}{dt} = \frac{1}{16\pi^2}\beta_\lambda^{(1)} + \frac{1}{(16\pi^2)^2}\beta_\lambda^{(2)}, \qquad \text{(A14)}$$

where the one-loop contribution is given by

$$\beta_\lambda^{(1)} = 12\lambda^2 - \left(\frac{9}{5}g_1^2 + 9g_2^2\right)\lambda + \frac{9}{4}\left(\frac{3}{25}g_1^4 + \frac{2}{5}g_1^2 g_2^2 + g_2^4\right) + 4Y_2(S)\lambda - 4H(S), \qquad \text{(A15)}$$

with

$$H(S) = \mathrm{Tr}\{3(\mathbf{Y}_u{}^\dagger \mathbf{Y}_u)^2 + 3(\mathbf{Y}_d{}^\dagger \mathbf{Y}_d)^2 + (\mathbf{Y}_e{}^\dagger \mathbf{Y}_e)^2\}, \qquad \text{(A16)}$$

and the two-loop contribution is given by [58]

$$\begin{aligned}
\beta_\lambda^{(2)} = &-78\lambda^3 + 18\left(\frac{3}{5}g_1^2 + 3g_2^2\right)\lambda^2 - \left[\left(\frac{313}{8} - 10n_g\right)g_2^4 - \frac{117}{20}g_1^2 g_2^2 + \frac{9}{25}\left(\frac{229}{4} + \frac{50}{9}n_g\right)g_1^4\right]\lambda \\
&+ \left(\frac{497}{8} - 8n_g\right)g_2^6 - \frac{3}{5}\left(\frac{97}{24} + \frac{8}{3}n_g\right)g_1^2 g_2^4 - \frac{9}{25}\left(\frac{239}{24} + \frac{40}{9}n_g\right)g_1^4 g_2^2 - \frac{27}{125}\left(\frac{59}{24} + \frac{40}{9}n_g\right)g_1^6 \\
&- 64g_3^2\mathrm{Tr}\{(\mathbf{Y}_u{}^\dagger \mathbf{Y}_u)^2 + (\mathbf{Y}_d{}^\dagger \mathbf{Y}_d)^2\} - \frac{8}{5}g_1^2\mathrm{Tr}\{2(\mathbf{Y}_u{}^\dagger \mathbf{Y}_u)^2 - (\mathbf{Y}_d{}^\dagger \mathbf{Y}_d)^2 + 3(\mathbf{Y}_e{}^\dagger \mathbf{Y}_e)^2\} - \frac{3}{2}g_2^4 Y_4(S) \\
&+ 10\lambda\left[\left(\frac{17}{20}g_1^2 + \frac{9}{4}g_2^2 + 8g_3^2\right)\mathrm{Tr}\{\mathbf{Y}_u{}^\dagger \mathbf{Y}_u\} + \left(\frac{1}{4}g_1^2 + \frac{9}{4}g_2^2 + 8g_3^2\right)\mathrm{Tr}\{\mathbf{Y}_d{}^\dagger \mathbf{Y}_d\} + \frac{3}{4}(g_1^2 + g_2^2)\mathrm{Tr}\{\mathbf{Y}_e{}^\dagger \mathbf{Y}_e\}\right] \\
&+ \frac{3}{5}g_1^2\left[\left(-\frac{57}{10}g_1^2 + 21g_2^2\right)\mathrm{Tr}\{\mathbf{Y}_u{}^\dagger \mathbf{Y}_u\} + \left(\frac{3}{2}g_1^2 + 9g_2^2\right)\mathrm{Tr}\{\mathbf{Y}_d{}^\dagger \mathbf{Y}_d\} + \left(-\frac{15}{2}g_1^2 + 11g_2^2\right)\mathrm{Tr}\{\mathbf{Y}_e{}^\dagger \mathbf{Y}_e\}\right] \\
&- 24\lambda^2 Y_2(S) - \lambda H(S) + 6\lambda\mathrm{Tr}\{\mathbf{Y}_u{}^\dagger \mathbf{Y}_u \mathbf{Y}_d{}^\dagger \mathbf{Y}_d\} + 20\mathrm{Tr}\{3(\mathbf{Y}_u{}^\dagger \mathbf{Y}_u)^3 + 3(\mathbf{Y}_d{}^\dagger \mathbf{Y}_d)^3 + (\mathbf{Y}_e{}^\dagger \mathbf{Y}_e)^3\} \\
&- 12\,\mathrm{Tr}\{\mathbf{Y}_u{}^\dagger \mathbf{Y}_u(\mathbf{Y}_u{}^\dagger \mathbf{Y}_u + \mathbf{Y}_d{}^\dagger \mathbf{Y}_d)\mathbf{Y}_d{}^\dagger \mathbf{Y}_d\}.
\end{aligned} \qquad \text{(A17)}$$

The β function for the vacuum expectation value of the scalar field is

$$\frac{d\ln v}{dt} = \frac{1}{16\pi^2}\gamma^{(1)} + \frac{1}{(16\pi^2)^2}\gamma^{(2)}, \qquad \text{(A18)}$$

where the one-loop contribution is given by

$$\gamma^{(1)} = \frac{9}{4}\left(\frac{1}{5}g_1^2 + g_2^2\right) - Y_2(S), \qquad \text{(A19)}$$

and the two-loop contribution is given by

$$\gamma^{(2)} = -\frac{3}{2}\lambda^2 - \frac{5}{2}Y_4(S) + \chi_4(S) - \frac{27}{80}g_1^2 g_2^2$$
$$- \left(\frac{93}{800} + \frac{1}{2}n_g\right)g_1^4 + \left(\frac{511}{32} - \frac{5}{2}n_g\right)g_2^4. \qquad \text{(A20)}$$

These expressions were arrived at using the general formulas provided in Ref. [7] for the anomalous dimension of the scalar field, choosing the Landau gauge.

In the low-energy regime the effective theory is $SU(3)_C \times U(1)_{em}$. We employ the general formula of Ref. [53] to arrive at the β functions for the respective gauge couplings:

$$\frac{dg_3}{dt} = \left(\frac{2}{3}(n_u + n_d) - 11\right)\frac{g_3^3}{(4\pi)^2} + \left(\frac{38}{3}(n_u + n_d) - 102\right)\frac{g_3^5}{(4\pi)^4} + \left(\frac{8}{9}n_u + \frac{2}{9}n_d\right)\frac{g_3^3 e^2}{(4\pi)^4}$$

$$+ \left(\frac{5033}{18}(n_u + n_d) - \frac{325}{54}(n_u + n_d)^2 - \frac{2857}{2}\right)\frac{g_3^7}{(4\pi)^6} , \tag{A21}$$

and

$$\frac{de}{dt} = \left(\frac{16}{9}n_u + \frac{4}{9}n_d + \frac{4}{3}n_l\right)\frac{e^3}{(4\pi)^2}$$

$$+ \left(\frac{64}{27}n_u + \frac{4}{27}n_d + 4n_l\right)\frac{e^5}{(4\pi)^4}$$

$$+ \left(\frac{64}{9}n_u + \frac{16}{9}n_d\right)\frac{e^3 g_3^2}{(4\pi)^4} , \tag{A22}$$

where n_u, n_d, and n_l are the number of up-type quarks, down-type quarks, and leptons, respectively. In Eq. (A21) we have also included the three-loop pure QCD contribution to the β function of g_3 [54].

For the evolution of the fermion masses we used Ref. [55]. It is known that there is an error in their printed formula [56]. Using the corrected expression, we compute the following mass anomalous dimension. The fermion masses in the low-energy theory then evolve as

$$\frac{dm}{dt} = \gamma_{(l,q)}m , \tag{A23}$$

where l and q refer to a particular lepton or quark, and where

$$\gamma_{(l,q)} = \gamma_{(l,q)}^1\frac{e^2}{(4\pi)^2} + \gamma_{(l,q)}^3\frac{g_3^2}{(4\pi)^2}$$

$$+ \frac{1}{(4\pi)^4}[\gamma_{(l,q)}^{11}e^4 + \gamma_{(l,q)}^{33}g_3^4 + 2\gamma_{(l,q)}^{13}e^2 g_3^2]$$

$$+ \gamma_{(q)}^{333}\frac{g_3^6}{(4\pi)^6} . \tag{A24}$$

The superscripts 1 and 3 refer to the $U(1)_{em}$ and $SU(3)_C$ contributions, respectively. Explicitly, the above coefficients are given by

$$\gamma_{(l,q)}^1 = -6Q_{(l,q)}^2,$$

$$\gamma_{(l)}^3 = 0,$$

$$\gamma_{(q)}^3 = -8,$$

$$\gamma_{(l)}^{13} = \gamma_{(l)}^{33} = 0,$$

$$\gamma_{(l,q)}^{11} = -3Q_{(l,q)}^4 + \left(\frac{80}{9}n_u + \frac{20}{9}n_d + \frac{20}{3}n_l\right)Q_{(l,q)}^2, \tag{A25}$$

$$\gamma_{(q)}^{13} = -4Q_{(q)}^2,$$

$$\gamma_{(q)}^{33} = -\frac{404}{3} + \frac{40}{9}(n_u + n_d),$$

$$\gamma_{(q)}^{333} = \frac{2}{3}\left[\frac{140}{27}(n_u + n_d)^2\right.$$

$$\left. + \left(160\zeta(3) + \frac{2216}{9}\right)(n_u + n_d) - 3747\right] ,$$

where $Q_{(l,q)}$ is the electric charge of a given lepton or quark, and $\zeta(3) = 1.2020569\ldots$ is the Riemann zeta function evaluated at three. In the mass anomalous dimension for the quarks above, we have also included the three-loop pure QCD contribution $\gamma_{(q)}^{333}$ [54].

APPENDIX B: EXPLICIT FORM OF $\delta(\mu)$

In Ref. [47] the radiative corrections term $\delta(\mu)$ from Eq. (2.76) is derived. In this appendix, we present its explicit form as it appears in this reference except for some minor notational changes. In the following, s and c refer to $\sin\theta_W$ and $\cos\theta_W$, respectively. Also, ξ is defined to be the ratio M_H^2/M_Z^2:

$$\delta(\mu) = \frac{G_\mu}{\sqrt{2}}\frac{M_Z^2}{8\pi^2}\{\xi f_1(\xi, \mu) + f_0(\xi, \mu) + \xi^{-1}f_{-1}(\xi, \mu)\} , \tag{B1}$$

where the various functions are defined as

$$f_1(\xi, \mu) = 6\ln\frac{\mu^2}{M_H^2} + \frac{3}{2}\ln\xi - \frac{1}{2}Z\left(\frac{1}{\xi}\right) - Z\left(\frac{c^2}{\xi}\right) - \ln c^2 + \frac{9}{2}\left(\frac{25}{9} - \frac{\pi}{\sqrt{3}}\right) ,$$

$$f_0(\xi, \mu) = -6\ln\frac{\mu^2}{M_Z^2}\left[1 + 2c^2 - 2\frac{M_t^2}{M_Z^2}\right] + \frac{3c^2\xi}{\xi - c^2}\ln\frac{\xi}{c^2} + 2Z\left(\frac{1}{\xi}\right) + 4c^2 Z\left(\frac{c^2}{\xi}\right) + \frac{3c^2\ln c^2}{s^2}$$

$$+ 12c^2\ln c^2 - \frac{15}{2}(1 + 2c^2) - 3\frac{M_t^2}{M_Z^2}\left[2Z\left(\frac{M_t^2}{M_Z^2\xi}\right) + 4\ln\frac{M_t^2}{M_Z^2} - 5\right] , \tag{B2}$$

$$f_{-1}(\xi, \mu) = 6\ln\frac{\mu^2}{M_Z^2}\left[1 + 2c^4 - 4\frac{M_t^4}{M_Z^4}\right] - 6Z\left(\frac{1}{\xi}\right) - 12c^4 Z\left(\frac{c^2}{\xi}\right) - 12c^4\ln c^2 + 8(1 + 2c^4)$$

$$+ 24\frac{M_t^4}{M_Z^4}\left[\ln\frac{M_t^2}{M_Z^2} - 2 + Z\left(\frac{M_t^2}{M_Z^2\xi}\right)\right] ,$$

with

$$Z(z) = \begin{cases} 2A\arctan(1/A) & (z > \tfrac{1}{4}), \\ A\ln[(1+A)/(1-A)] & (z < \tfrac{1}{4}), \end{cases}$$

$$A \equiv |1 - 4z|^{\frac{1}{2}} .$$

(B3)

APPENDIX C: NUMERICAL TECHNIQUES

We use the Runge-Kutta method to numerically integrate the β functions. There are 18 coupled first order differential equations involved in running the standard model couplings. At one loop some equations decouple from the rest. For example, the gauge couplings are decoupled at one loop. However, the Yukawa β functions depend on both gauge couplings and Yukawa couplings even at one loop as in Eqs. (A8)–(A10). We are working with two-loop β functions and these are all coupled. Standard Runge-Kutta programs are readily available; however, these usually assume knowledge of initial values of all couplings at the same scale t_0, where t will denote the scaling parameter. This presents somewhat of a problem since different couplings may be known at significantly different scales.

The method we employ to solve the initialization problem is often referred to as "shooting" [57]. Simply put, a guess is made for the initial values of all the parameters at the chosen scale, t_0. The parameters are then evolved to the various scales where one has known values, and the merits of the guess are assessed. The procedure is optimized, and one thereby arrives at a solution. Arriving at initial values of the couplings at the same initial scale therefore involves the solution of a possible 18 non-linear equations in 18 unknowns. That is, in the most general case, if it is assumed that none of the parameters are known at the desired initial scale t_0, then 18 coupled functions of 18 variables can be defined as

$$F_i(\mathbf{x}(t_0)) = RK\{\mathbf{x}(t_0); t_i\}_i - X_i ,$$

(C1)

where $\mathbf{x}(t_0)$ is an 18 component vector denoting the unknown parameters at t_0, X_i is the known (possibly experimentally determined) value of the ith parameter at some scale t_i, and $RK\{\mathbf{x}(t_0); t_i\}_i$ is the value of the ith parameter resulting from numerically integrating the β evolution equations to a scale t_i given initial values, $\mathbf{x}(t_0)$ at t_0. Solution routines that solve N simultaneous non-

linear equations in N unknowns, that is, they solve

$$F_i(\mathbf{x}(t_0)) = 0 ,$$

(C2)

are then used to find $\mathbf{x}(t_0)$. In our case $x_i(t_0)$, $i = 1, ..., 18$, represent the 18 parameters of the standard model, and we have chosen the initial scale $\mu_0 = e^{t_0} = M_Z$. Our task has been appreciably simplified since we have most initial data at M_Z. Only the fermion masses are taken at a different scale. This reduces the number of simultaneous equations and therefore the computing task.

As the top-quark and Higgs-boson masses are unknown in the standard model at present, in the process of our analyses we are free to choose values for these masses at M_Z and then proceed to study the consequences. In other models in which there may be certain constraints (e.g., in some GUT's the b and τ Yukawa couplings are equal at the scale of grand unification), one may incorporate these constraints into the functions (C2). The freedom to choose a value for an unknown parameter may be replaced by such a constraint, and this may result in a definite prediction for that parameter. Constraints from grand unification and supersymmetry were used in Ref. [5] to arrive at possible values for the top-quark and Higgs-boson masses.

After all data is obtained at M_Z by employing the initialization procedure described above, the Runge-Kutta routines are used to evolve the parameters to any mass scale μ. We have provided several figures (3–7) displaying the evolution of many of the parameters of the standard model for the case $m_t(M_Z) = 95$ GeV. As discussed in Sec. II G, given the evolution of the running parameters m_t and λ, the physical top-quark and Higgs-boson masses may be found by solving Eqs. (2.75) and (2.76). These equations are solved using the nonlinear equation solution routines described above in the initialization procedure. For example, consider the above situation in which $m_t(M_Z) = 95$ GeV, and suppose we wish to find the corresponding physical mass M_t in this case. The solution algorithm may be described as follows: A guess is made for M_t, then the running parameters are evolved using the Runge-Kutta routine to this mass scale (i.e., $\mu = M_t$). The guess is tolerated depending on how accurately one wishes Eq. (2.75) to be satisfied when values for $\alpha_s(M_t)$ and $m_t(M_t)$ are substituted. The solution routines effectively optimize this shooting or guessing procedure and yield a value for M_t corresponding to the value $m_t(M_Z)$. In this particular case, the result is $M_t = 100$ GeV.

[1] J. C. Pati and A. Salam, Phys. Rev. D **10**, 275 (1974); H. Georgi and S. Glashow, Phys. Rev. Lett. **32**, 438 (1974); H. Georgi, in *Particles and Fields-1974* (APS/DPF Williamsburg), Proceedings of the 1974 Meeting of the APS Division of Particles and Fields, edited by C. A. Carlson, AIP Conf. Proc. No. 23 (AIP, New York, 1975), p. 575; H. Fritzsch and P. Minkowski, Ann. Phys. (N.Y.) **93**, 193 (1975); F. Gürsey, P. Ramond, and P. Sikivie, Phys. Lett. **60B**, 177 (1975).

[2] H. Georgi, H. Quinn, and S. Weinberg, Phys. Rev. Lett.

33, 451 (1974).

[3] N. Cabibbo, L. Maiani, G. Parisi, and P. Petronzio, Nucl. Phys. **B158**, 295 (1979).

[4] U. Amaldi, W. de Boer, and H. Fürstenau, Phys. Lett. B **260**, 447 (1991).

[5] H. Arason, D. J. Castaño, B. Keszthelyi, S. Mikaelian, E. J. Piard, P. Ramond, and B. D. Wright, Phys. Rev. Lett. **67**, 2933 (1991).

[6] S. Kelley, J. L. Lopez, and D. V. Nanopoulos, Phys. Lett. B **274**, 387 (1992).

[7] M. E. Machacek and M. T. Vaughn, Nucl. Phys. **B222**, 83 (1983); **B236**, 221 (1984); **B249**, 70 (1985).

[8] W. J. Marciano, in *The Santa Fe TASI*, Proceedings of the Theoretical Advanced Study Institute in Elementary Particle Physics, Santa Fe, New Mexico, 1987, edited by R. Slansky and G. West (World Scientific, Singapore, 1988).

[9] R. D. Peccei, in *The Standard Model and Beyond*, Proceedings of the Fifth Lake Louise Winter Institute, Chateau Lake Louise, Canada, 1990, edited by A. Astbury *et al.* (World Scientific, Singapore, 1990).

[10] D. A. Ross, Nucl. Phys. **B140**, 1 (1978); T. J. Goldman and D. A. Ross, Phys. Lett. **84B**, 208 (1979).

[11] S. Weinberg, Phys. Lett. **91B**, 51 (1980).

[12] L. Hall, Nucl. Phys. **B178**, 75 (1981).

[13] B. A. Ovrut and H. J. Schnitzer, Phys. Rev. D **21**, 3369 (1980); **22**, 2518 (1980); Nucl. Phys. **B179**, 381 (1981); **B184**, 109 (1981); Phys. Lett. **100B**, 403 (1981).

[14] C. H. Llewellyn Smith, G. G. Ross, and J. F. Wheater, Nucl. Phys. **B177**, 263 (1981).

[15] G. 't Hooft, Nucl. Phys. **B61**, 455 (1973).

[16] W. A. Bardeen, A. J. Buras, D. W. Duke, and T. Muta, Phys. Rev. D **18**, 3998 (1978).

[17] W. Marciano and A. Sirlin, Phys. Rev. Lett. **46**, 163 (1981).

[18] A. Sirlin, Phys. Rev. D **22**, 971 (1980).

[19] W. Marciano, Phys. Rev. D **20**, 274 (1979).

[20] W. J. Marciano and A. Sirlin, Phys. Rev. D **22**, 2695 (1980).

[21] S. Sarantakos, A. Sirlin, and W. Marciano, Nucl. Phys. **B217**, 84 (1983).

[22] A. Sirlin, Phys. Lett. B **232**, 123 (1989).

[23] S. Fanchiotti and A. Sirlin, Phys. Rev. D **41**, 319 (1990).

[24] Particle Data Group, J. J. Hernández *et al.*, Phys. Lett. B **239**, 1 (1990).

[25] G. Altarelli, *The Rice Meeting*, Annual Meeting of the Division of Particles and Fields of the APS, Houston, Texas, 1990, edited by B. Bonner and H. E. Miettinen (World Scientific, Singapore, 1990), pp. 170–206.

[26] S. G. Gorishny, A. L. Kataer, and S. A. Lavin, Phys. Lett. B **259**, 144 (1989).

[27] H. Wachsmuth, in *The Vancouver Meeting—Particles and Fields '91*, Proceedings of the Joint Meeting of the Division of Particles and Fields of the American Physical Society and the Particle Physics Division of the Canadian Association of Physicists, Vancouver, 1991, edited by D. Axen, D. Bryman, and M. Comyn (World Scientific, Singapore, 1992).

[28] W. Kwong, P. B. Mackenzie, R. Rosenfeld, and J. L. Rosner, Phys. Rev. D **37**, 3210 (1988).

[29] A. D. Martin, R. G. Roberts, and W. J. Stirling, Phys. Rev. D **43**, 3648 (1991).

[30] A. Ali and F. Barreiro, in *High Energy Electron-Positron Physics*, edited by A. Ali and P. Soding (World Scientific, Singapore, 1988), p. 611.

[31] J. Ellis, D. V. Nanopoulos, and D. A. Ross, Phys. Lett. B **269**, 132 (1991).

[32] F. Anselmo, L. Cifarelli, A. Petermann, and A. Zichichi, Nuovo Cimento A **104**, 1817 (1991).

[33] A slightly different analysis in Ref. [31] yields the same value.

[34] J. Gasser and H. Leutwyler, Phys. Rep. **87**, 77 (1982).

[35] S. Narison, Phys. Lett. B **216**, 191 (1989).

[36] S. Narison, *QCD Spectral Sum Rules* (World Scientific, Singapore, 1989).

[37] M. G. Olsson, University of Wisconsin-Madison Report No. MAD/PH/656, 1991 (unpublished).

[38] E. Braaten, S. Narison, and A. Pich, Nucl. Phys. **B373**, 581 (1992).

[39] N. Gray, D. J. Broadhurst, W. Grafe, and K. Schilcher, Z. Phys. C **48**, 673 (1990).

[40] M. A. Shifman, A. I. Vainshtein, and V. I. Zakharov, Nucl. Phys. **B147**, 385 (1979).

[41] C. A. Dominguez and E. de Rafael, Ann. Phys. (N.Y.) **174**, 372 (1987).

[42] S. Narison and E. de Rafael, Phys. Lett. **103B**, 57 (1981).

[43] C. A. Dominguez, C. van Gend, and N. Paver, Phys. Lett. B **253**, 241 (1991).

[44] P. Langacker and M. Luo, Phys. Rev. D **44**, 817 (1991).

[45] J. Ellis and G. L. Fogli, Phys. Lett. B **249**, 543 (1990).

[46] ALEPH Collaboration, D. Decamp *et al.*, CERN Report No. CERN-PPE/91-19, 1991 (unpublished).

[47] A. Sirlin and R. Zucchini, Nucl. Phys. **B266**, 389 (1986).

[48] W. Marciano, Annu. Rev. Nucl. Part. Sci. **41**, 469 (1991).

[49] F. Antonelli and L. Maiani, Nucl. Phys. **B186**, 269 (1981).

[50] J. F. Wheater and C. H. Llewellyn Smith, Nucl. Phys. **B208**, 27 (1982).

[51] T. Appelquist and J. Carazzone, Phys. Rev. D **11**, 2856 (1975).

[52] W. J. Marciano, Phys. Rev. D **29**, 580 (1984).

[53] D. R. T. Jones, Phys. Rev. D **25**, 581 (1982).

[54] O. V. Tarasov, A. A. Vladimirov, and A. Y. Zharkov, Phys. Lett. **93B**, 429 (1980); S. G. Gorishny, A. L. Kataev, and S. A. Larin, Yad. Fiz. **40**, 517 (1984) [Sov. J. Nucl. Phys. **40**, 329 (1984)].

[55] D. V. Nanopoulos and D. A. Ross, Nucl. Phys. **B157**, 273 (1979).

[56] R. Tarach, Nucl. Phys. **B183**, 384 (1981).

[57] One of us (D.J.C.) is grateful to Professor James Nearing of the University of Miami Physics Department for pointing out this method of solving the problem.

[58] We correct here discrepancies in the $\lambda g_1^2 g_2^2$ and λg_1^4 terms of Machacek and Vaughn [7]. We became aware of these errors in Ref. [59], where the correct formula recently calculated in Ref. [60] is also presented. These errors in the two-loop formula, however, have very little numerical effect on our results.

[59] V. Barger, M. S. Berger, and P. Ohmann, University of Wisconsin-Madison Report No. MAD/PH/711, 1992 (unpublished).

[60] C. Ford, I. Jack, and D. R. T. Jones, DAMTP and ITP-Santa Barbara Report No. NSF-ITP-92-21, 1992 (unpublished). This paper also contains the two-loop β function of the m^2 of the Higgs boson of the standard model.